

2013

Scaffold Composition and Architecture Critically Regulate Extracellular Matrix Synthesis by Cardiomyocytes

Arsela Gishto
Cleveland State University

Follow this and additional works at: <https://engagedscholarship.csuohio.edu/etdarchive>

 Part of the [Biomedical Engineering and Bioengineering Commons](#)

How does access to this work benefit you? Let us know!

Recommended Citation

Gishto, Arsela, "Scaffold Composition and Architecture Critically Regulate Extracellular Matrix Synthesis by Cardiomyocytes" (2013). *ETD Archive*. 812.
<https://engagedscholarship.csuohio.edu/etdarchive/812>

This Thesis is brought to you for free and open access by EngagedScholarship@CSU. It has been accepted for inclusion in ETD Archive by an authorized administrator of EngagedScholarship@CSU. For more information, please contact library.es@csuohio.edu.

**SCAFFOLD COMPOSITION AND ARCHITECTURE CRITICALLY REGULATE
EXTRACELLULAR MATRIX SYNTHESIS BY CARDIOMYOCYTES**

ARSELA GISHTO

Bachelors of Science in Biology

Bachelors of Science in Health Sciences

Cleveland State University

May 2011

Submitted in partial fulfillment of requirements for the degree

MASTER OF SCIENCE IN BIOMEDICAL ENGINEERING

at

CLEVELAND STATE UNIVERSITY

December 2013

We hereby approve this thesis of

Arsela Gishto

Candidate for the Master of Science in Biomedical Engineering degree for the

Department of Chemical and Biomedical Engineering

and the CLEVELAND STATE UNIVERSITY
College of Graduate Studies

Thesis Chairperson, Dr. Chandra Kothapalli
Department of Chemical and Biomedical Engineering

Date

Thesis Committee Member, Dr. Joanne Belovich
Department of Chemical and Biomedical Engineering

Date

Thesis Committee Member, Dr. Moo-Yeal Lee
Department of Chemical and Biomedical Engineering

Date

Friday, December 6, 2013

ACKNOWLEDGMENTS

I would first like to thank my advisor, Dr. Chandra Kothapalli for his support and guidance. Specifically, Dr. Kothapalli was an indispensable resource due to his breadth of knowledge in cardiac tissue engineering and routine advice and positive encouragement. I would like to acknowledge all my committee members, Dr. Joanne Belovich, Dr. Moo-Yeal Lee and Dr. Srividya Sundararaman for their support.

I would like to recognize my fellow colleagues at Cleveland State University, including Kurt Farrell for teaching me many laboratory procedures, helping with SEM imaging, and always being available and ready to help, as well as the rest of the Tissue engineering lab group: Phillip Simmers, Jyotsna Joshi, Amanda Powell, and Sameera Tasneem. The Biomedical and Chemical engineering staff at Cleveland State University including Jim Barker for helping with SEM imaging and Becky Laird and Darlene Montgery for their aid and guidance.

I would like to recognize financial support from Trio Student Support Services under the direction of George Bovell, as well as tuition support from The Choose Ohio First Scholarship program.

Lastly, I would like to thank my mother, Adriana Gishto, my father, Ramadan Gishto, my brother, Ermal Gishto and my fiancé, Jamal Chehab for always believing in me and constantly supporting me in every step of my scientific and academic endeavors.

SCAFFOLD COMPOSITION AND ARCHITECTURE CRITICALLY REGULATE EXTRACELLULAR MATRIX SYNTHESIS BY CARDIOMYOCYTES

ARSELA GISHTO

ABSTRACT

Heart failure accounts for over 5 million cases in the U.S. A major onset of this is myocardial infarction, which causes the myocardium to lose cardiomyocytes and transform into a scar tissue. Given that the adult infarcted cardiac tissue has a limited ability to regenerate, alternative methods to restore the damaged area need to be developed. The goal of these approaches is to design an optimal scaffold that can retain and deliver cardiomyocytes at the site of damaged myocardium. This tissue engineering approach would allow cardiac reconstruction by replacing the lost cardiomyocytes, delivering the required biomolecules, as well as remodeling the extracellular matrix (ECM). In this study we investigate the effects of a variety of ECM substrates on the attachment, survival and ECM production by cardiomyocytes. We cultured rat cardiomyocytes for 21 days in eleven different substrates, including nanofiber coated plates and 3D hydrogels. Cell attachment and survival rates were analyzed both quantitatively and qualitatively. ELISA and fluorometric assays were performed to quantify the synthesis and release of ECM protein molecules by the cells under various culture conditions. The matrix protein deposition was also qualitatively analyzed using immunofluorescence staining and imaging. Finally, the production of MMPs-2, 9 and

TIMP-1 by these cells was quantified and correlated to matrix synthesis under respective culture conditions. The observations of this study were that the total protein content quantified within PCL nanofiber scaffolds was significantly higher compared to that within hydrogels. Collagen concentration played an important role in cardiomyocyte survival. Among all cases tested, 2 mg/ml collagen-I (CI-2) provided the highest cell survival rate. Additionally, laminin-coated PCL nanofiber scaffold provided the most suitable environment for cardiomyocytes to result in the highest number of beating cardiomyocytes. However, the maximum beating frequencies were noted in cells cultured on collagen I and collagen IV coated scaffolds. Taken together, our results suggest that 3D scaffold composition and architecture influences cardiomyocyte phenotype and matrix protein synthesis, with significant applications in cardiac tissue engineering and regeneration.

TABLE OF CONTENTS

	Page
ABSTRACT.....	iv
LIST OF TABLES.....	ix
LIST OF FIGURES.....	x
CHAPTER.....	1
I. INTRODUCTION.....	1
II. BACKGROUND.....	5
2.1 Myocardium organization and myocardial infarction (MI).....	5
2.2 Surgical and pharmacological approaches for MI treatment.....	8
2.3 Tissue engineering approaches.....	9
2.3.1 2D substrates.....	11
2.3.2 3D scaffolds.....	12
2.3.3 In vivo studies.....	15
2.4 Myocardial extracellular matrix.....	16
III. MATERIALS AND METHODS.....	23
3.1 Scaffold preparation.....	23
3.2 Rat cardiomyocytes culture.....	25
3.3 Live/Dead Viability/Cytotoxicity assay.....	26
3.4 Biochemical analysis.....	27
3.5 Immunofluorescence analysis.....	33
3.6 Scanning electron microscopy.....	34
3.7 Contractile properties of R-CM in PCL nanofiber scaffolds.....	35

3.8 Statistical analysis.....	35
IV. RESULTS AND DISCUSSION.....	36
4.1 Hydrogel scaffolds.....	36
4.1.1 Live/Dead Viability/Cytotoxicity assay.....	36
4.1.2 Biochemical analysis.....	38
4.1.3 Immunofluorescence analysis.....	44
4.2 PCL nanofiber coated scaffolds.....	47
4.2.1 Live/Dead Viability/Cytotoxicity assay.....	47
4.2.2 Biochemical analysis.....	48
4.2.3 Immunofluorescence analysis.....	53
4.2.4 Scanning electron microscopy.....	54
4.2.5 Beating cardiomyocytes.....	55
V. CONCLUSIONS AND RECOMMENDATIONS.....	56
5.1 Conclusions.....	56
5.2 Recommendations.....	58
BIBLIOGRAPHY.....	60

LIST OF TABLES

Table	Page
3.1 Scaffold compositions with respective notations.....	24
3.2 Summary of antibodies used for immunofluorescence analysis.....	34

LIST OF FIGURES

Figure	Page
2.1 (A) Cardiac muscle composed of endocardium, myocardium and epicardium. (B) 3D structure of cardiomyocytes surrounded by endomysium and perimysium ⁸	6
2.2 Immunofluorescence staining of myocardium for Poly(ADP-ribose) (PAR), an indicator of PARP activation ¹¹	7
2.3 Three different treatment options for myocardial infarction. Polymer meshes sutured around the heart to (a) prevent further damage in the left ventricular (LV) (b) maintain the structure of LV. (c) Cultured cells on a biomaterial scaffold in vitro and implanted onto the epicardial surface (d) A biomaterial injected in situ (e) A scaffold injected in situ delivering cells, growth factors ¹⁰	10
2.4 The architecture of the main proteins found in the cardiac tissue.....	17
2.5 Structure of ECM molecules. (A) Fibronectin dimer; polypeptides linked by disulfide bonds. (B) Laminin composed of three different polypeptides chains linked by disulfide bonds. (C) Sulfated repeating disaccharide unit of GAGs. (D) Non-sulfated GAG disaccharide unit ³² . (E) Elastic fiber assembly: (1) tropoelastin cross-linked by LOX to form elastin polymer, (2) elastin polymer on the cell surface, (3) elastin polymers transferred to microfibrils through integrins, (4) larger elastin polymer formation, (5) Elastin polymer cross-linked by LOX to form final elastin protein ³⁶	20
4.1 The percentage survival rate of rat cardiomyocytes at the end of 21 day culture, obtained from Live/Dead Viability assay (n=2). Data was shown as mean \pm standard error.....	38
4.2 Protein syntheses by rat cardiomyocytes at the end of 21 day culture (n=3). Data was	

shown as mean \pm standard error. (A) Total protein synthesized in cell matrix and released in pooled media on a per cell basis, obtained from BCA protein assay. (B) Amount of sGAGs synthesized in cell matrix and released in pooled media on a per cell basis, obtained from sGAG assay. (C) HA content released in pooled media on a per cell basis, obtained by HA ELISA assay. (D) Elastin synthesized in cell matrix and released in pooled media on a per cell basis, obtained by Fastin Elastin assay. (E) LOX content released in pooled media on a per cell basis, obtained by Amplex® Red Hydrogen Peroxide/Peroxidase assay.....	40
4.3 Quantification of MMPs and TIMP expressed by rat cardiomyocytes at the end of 21 day culture (n=3). Data was shown as mean \pm standard error. (A) MMP-2 content in pooled media on a per cell basis obtained by MMP-2 assay. (B) MMP-9 released in pooled media on a per cell basis obtained by MMP-9 assay. (C) TIMP-1 content in pooled media on a per cell basis obtained by TIMP-1 assay.....	43
4.4 Immunofluorescence images showing staining of rat cardiomyocytes at day 21 for Elastin, Fibrillin and LOX. (n=2; 40x magnification; scale bar = 40 μ m).....	45
4.5 Immunofluorescence images showing the α -Actinin and ELR staining of rat cardiomyocytes at day 21. Nuclei are DAPI stained blue. (n=2; 40x magnification; scale bar = 40 μ m).....	46
4.6 The percentage survival rate of rat cardiomyocytes at the end of 21 day culture, obtained from Live/Dead Viability assay (n=2). Data was shown as mean \pm standard error.....	47
4.7 Proteins expressed by rat cardiomyocytes at the end of 21 day culture (n=2). Data was shown as mean \pm standard error. (A) Total protein released in pooled media on a per cell	

basis, obtained from BCA protein assay. (B) Total protein synthesized in cell matrix on a per cell basis, obtained from BCA protein assay. (C) sGAGs synthesized in cell matrix and released in pooled media normalized to the total protein amount on a per cell basis, obtained from sGAG assay. (D) HA content in cell matrix and released in pooled media normalized to the total protein on a per cell basis, obtained by HA ELISA assay. (E) Elastin synthesized in cell matrix and released in pooled media normalized to the total protein amount on a per cell basis, obtained by Fastin Elastin assay. (F) LOX content in cell matrix and released in pooled media normalized to the total protein on a per cell basis, obtained by Amplex® Red Hydrogen Peroxide/Peroxidase assay.....	49
4.8 Quantification of MMPs and TIMP expressed by rat cardiomyocytes at the end of 21 day culture (n=3). Data was shown as mean \pm standard error. (A) MMP-2 content in pooled media on a per cell basis obtained by MMP-2 assay. (B) MMP-9 released in pooled media on a per cell basis obtained by MMP-9 assay. (C) TIMP-1 content in pooled media on a per cell basis obtained by TIMP-1 assay.....	52
4.9 Immunofluorescence images showing staining of rat cardiomyocytes at day 21 for Fibrillin, Elastin, and α -actinin. (n=2; 40x magnification; scale bar = 40 μ m).....	53
4.10 Immunofluorescence images showing staining of rat cardiomyocytes at day 21 for ELR and LOX. (n=2; 40x magnification; scale bar = 40 μ m).....	53
4.11 SEM images of rat cardiomyocytes cultured on PCL nanofiber scaffolds.....	54
4.12 (A) Percentage of beating cardiomyocytes over the 21 day culture in five various scaffolds. (B) Average beating frequency of the cardiomyocytes during the 21 day culture.....	55

CHAPTER I

INTRODUCTION

Cardiovascular disease (CVD) is the leading cause of mortality in the United States and it accounts for over 30% of deaths each year. According to the American Heart Association (AHA), 83.6 million adults suffer from at least one type of CVD in America. Besides this enormous number of patients diagnosed with CVD, there is an increase of 28% in treatment procedures in the recent years. This has resulted in a decline of death rate linked to CVD by 32.7% in a 10 year period (1999-2009). However, the cost attributed to CVD remains drastically high, over \$300 billion. The major contributors to CVD are hypertension, diabetes mellitus, obesity, increased levels of cholesterol and myocardial infarction (MI). MI is the leading cause of this high CVD mortality rate. Approximately 7.6 million of MI cases occur in the U.S. every year¹.

MI occurs as a result of ischemia, not enough blood and oxygen supplied to the myocardium. The infarcted myocardium suffers irreversible damages and loses its cells permanently. The cardiac muscle then transforms into a scar tissue which leads in an (ECM) reconstruction, loss of cardiac function, and eventually heart failure. The

myocardium does not have the ability to regenerate itself and replace the lost cardiomyocytes. Therefore alternative methods need to be developed to reconstruct the damaged cardiac tissue and its contractile function. One approach to repair the damaged myocardium is to replace the lost cardiomyocytes by delivering the required biomolecules, as well as remodeling the ECM. This tissue engineering approach allows the delivery of cardiomyocytes by placing a scaffold that mimics the natural cardiac micro-environment into the infarcted site. During this myocardial regeneration process, the scaffold needs to be physically and chemically suitable for cardiac myocytes attachment and survival^{2,3}.

Previous studies have shown that a 3-dimensional (3D) scaffold provides advantages in cell attachment and proliferation. Additionally, the chemical composition of the scaffold has a significant role in cell alignment and survival rate. Various types of synthetic [polycaprolactone (PCL), PCL\gelatin (PG), polyglycolic acid (PGA)] and biological scaffolds (gelatin, matrigelTM, laminin, collagen) have been developed and tested in vitro³⁻⁶. The synthetic 3D scaffolds can allow for an electrical communication and synchronized beating between cardiomyocytes⁷. Previous studies have shown that aligned nano-fiber scaffolds provide better mechanical properties compared to random non-aligned ones³. However these 3D scaffolds need to provide biocompatibility with the cardiac myocytes for higher tissue restoration results. To increase the biocompatibility, the polymer nanofibers can be combined with naturally occurring proteins. Furthermore ECM proteins fused together in a 3D architecture can simulate a suitable cardiac substrate. These tissue engineering approaches can be developed more with a better understanding of the ECM composites produced by cardiomyocytes. Unfortunately, there

is no reported data in literature which analyzed the amounts of ECM proteins synthesized and deposited by cardiomyocytes within various scaffolds.

To overcome these limitations, we designed this study with the following goals. The primary objective of this research is to study and understand the effects of scaffold composition, stiffness and architecture on cardiomyocyte attachment and survival. Additionally, the second aim of this study is to investigate the role of 3D scaffold characteristics on extracellular matrix synthesis and deposition by cardiomyocytes. The matrix molecules quantified in this project are hyaluronic acid (HA), elastin, sGAGs, LOX, MMPs-2 and 9, TIMP-1.

This thesis is organized as follows:

Chapter II provides an overview of the structure and function of the cardiac muscle and its extracellular matrix organization. Also, it provides a summary of the MI treatment options that are available and in progress, accompanied by a discussion of their limitations.

Chapter III describes the experimental procedures used for the in vitro culturing of cardiomyocytes in a variety of 3D biological scaffolds composed of ECM proteins (collagen types I and IV, laminin, fibronectin) and biodegradable nanofiber scaffolds (PCL) coated with the ECM proteins. Furthermore, this chapter provides a detailed description of the quantitative (ELISA and fluorometric assays) and qualitative (immunofluorescence staining and imaging) analysis of cell survival data and ECM molecules synthesized and released by the cardiomyocytes.

Chapter IV announces the results obtained from the experiments described in Chapter III and their interpretation.

Chapter V provides conclusions drawn from the results on Chapter IV and an overview of how the knowledge gained on 3D scaffold composition and matrix synthesis by cardiomyocytes can be used to design a suitable scaffold that optimizes the attachment and survival of cardiomyocytes and improves the cardiac function in cases of MI.

CHAPTER II

BACKGROUND

2.1 Myocardium organization and myocardial infarction

Myocardium is the intermediate layer of the cardiac muscle bordered by endocardium and epicardium (**Figure 2.1 A**). The myocardium is composed of contractile cardiomyocytes assembled in a 3 dimensional fiber network and interstitial space occupied by fibroblasts, endothelial cells, blood vessels, and ECM. Each individual cardiac myocyte is surrounded and supported by endomysium, a structure of fibrocollagenous connective tissue as shown in **Figure 2.1 B**. Perimysium, a connective tissue network that encircles bundles of myocytes, supports the shearing forces and alignment between them (**Figure 2.1 B**). Any damages in the myocardium reflect in changes in these supporting extracellular matrices⁸. An irreversible damage of the cardiac muscle can be caused by myocardial infarction (MI), also known as heart attack. MI is caused by a coronary artery blockage due to plaque build-up and thrombosis, blocking

blood flow to the muscle. The restriction of blood and oxygen supplied to the myocardium results in cardiomyocyte death, which unfortunately are difficult to replace or regenerate.

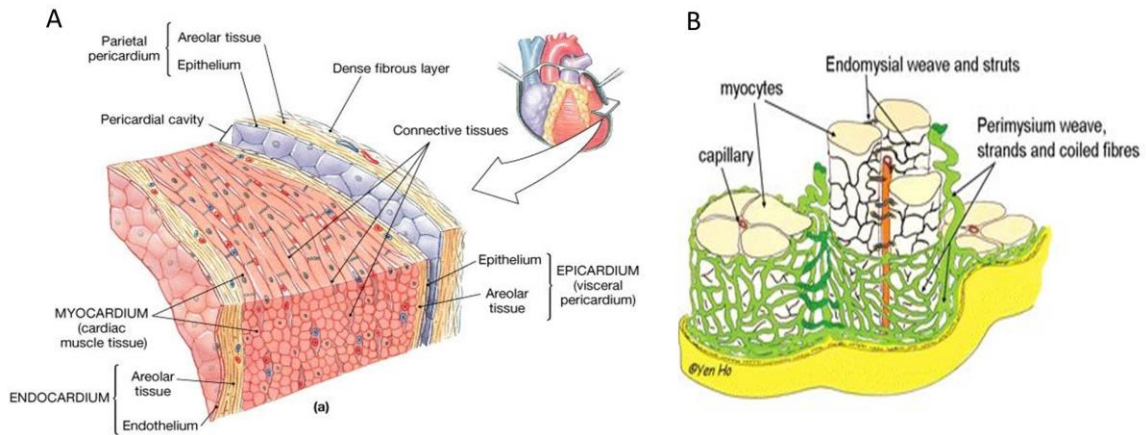


Figure 2.1 (A) Cardiac muscle composed of endocardium, myocardium and epicardium. **(B)** 3D structure of cardiomyocytes surrounded by endomysium and perimysium⁸.

During MI, the number of cardiomyocytes is drastically reduced in the infarcted area which results in a reduction of cardiac function⁹. The cell death in MI is followed by an inflammatory response caused by the migration of macrophages, monocytes, and neutrophils to the damaged area of the myocardium. This damage continues and expands with the production of matrix metalloproteinases that have the ability to degrade the ECM and could lead to an increase of irregular and disorganized collagen deposition. The ECM changes result in a non-elastic matrix trapping the cardiomyocytes and causing misalignment and impairment of electrical conductivity between the cells, causing a continuance in cell death. The lack of blood supply to the myocardium during acute MI

causes permanent necrosis and ECM remodeling. This is followed by the formation of scar tissue in the myocardium damaged area and eventually resulting in heart failure¹⁰.

Figure 2.2 shows the disturbance occurring in cellular level of the myocardium during MI. Studies has shown the presence of poly(ADP-ribose) polymerases (PARPs) during MI, which are activated during ischemia and continue to be deposited during MI¹¹. PARPs are responsible for the activation of inflammatory pathways and draining of cellular energetic pools which lead to cell necrosis¹¹. The inhibition of PARPs can be a first step in delaying and preventing chronic MI damages that can be life threatening. The infarcted zone needs to be treated and repaired properly to allow regain of normal physiology¹¹.

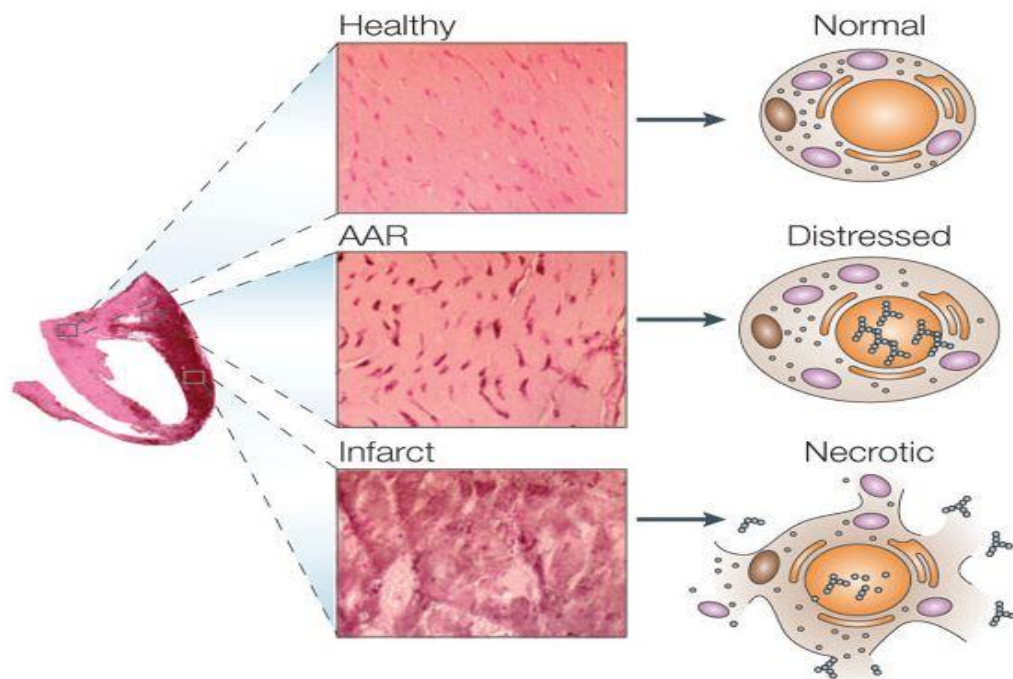


Figure 2.2 Immunofluorescence staining of myocardium for Poly(ADP-ribose) (PAR), an indicator of PARP activation. The healthy myocardium shows normal cells not stained for PAR. The area at risk (AAR) of MI shows severely distressed cells and PAR staining. Infarcted area shows necrotic myocytes with abundant PAR staining¹¹.

2.2 Surgical and pharmacological approaches for MI treatment

Due to the enormous number of CVD and heart failure cases, considerable research has been done for cardiac repair and cardiac muscle regeneration over the past decades. The primary option in decreasing MI prevalence is their prevention by controlling the underlying risks. In patients suffering from hypertension, high levels of cholesterol, obesity, diabetes mellitus, and/or that are genetically prone to cardiac issues, it is essential that they take the proper medications and follow the right lifestyle to keep their conditions under control. Other options to treat cardiac diseases and prevent further damages include drug delivery, use of certain devices and surgery. Depending on the factor that caused the cardiac dysfunction, the treatment options can vary.

Drug delivery is a method used to provide the required medications in the right dosage to treat certain conditions. Angiotensin-converting enzyme (ACE) inhibitor is one type of medication that can be used in cases of left ventricular systolic dysfunction or after the occurrence of acute MI to prevent or help manage heart failure¹². However this medication has many side effects such as renal insufficiency and hypertension. It can be combined with diuretic drugs to control fluid accumulation in patients with congestive heart failure. A wider range of cardiovascular conditions can be treated with beta-blocker medications that can reduce and prevent further symptoms when inhibited in the right dosage. A few other examples of drugs used in cardiac dysfunctions are nitrates, anti-thrombotic agents and nesiritide¹².

In cases of coronary artery disease, stents can be inserted to enlarge the blocked blood vessels. This procedure is known as angioplasty, but not always applicable in

vessels of smaller sizes. However, bypass surgery can be used as another treatment option by placing biological or synthetic vascular grafts in the damaged zone. This procedure has many limitations such as incompatibility issues¹³. Pacemakers are other devices that are used in cases of heart failure to normalize the heart rate and function. Although the placement of a pacemaker can cause dyssynchrony and further the damage, this can be resolved by using a bi-ventricular pacemaker. In cases of severe heart failure, the pacemakers are combined with defibrillators. However, they cannot be used within 40 days of the occurrence of myocardial infarction¹². Although pharmacological and surgical approaches contribute to improvements in cardiac output and functionality, they do not replace, restore or regenerate lost cells and tissue within the damaged or diseased region of the heart.

Heart transplantation is the last option that can be used in cases of end-stage heart failure. If the previously discussed treatment options prove to be unsuccessful, the transplantation of a new heart is the only left choice. However, there are a few issues linked with this option. One is the problem of finding a heart donor and the main issue is the rejection of a new foreign heart by the patient. This has led to a significant death rate within the first year after surgery. Despite their clinical usage and relevance, the above-mentioned treatment methods have many limitations; hence alternative strategies need to be developed for cardiac repair¹².

2.3. Tissue engineering approaches

The goal of current tissue engineering approaches is to improve biocompatibilities of prosthetic devices and grafts, and to design and develop biomaterials and cell delivery

options for cardiac repair and regeneration. Numerous studies have been done so far in the areas of suitable scaffold development, cell transplantation and stem cell based therapies, which can be used for treatment of MI. When myocardial damage has occurred, the main concern is to prevent the infarcted zone from enlarging which could lead to heart failure. **Figure 2.3** presents an overview of some techniques investigated for potential MI treatment. These tissue engineering approaches can be categorized into *in vitro* and *in situ* techniques. Cellular cardiomyoplasty is an *in situ* technique where cells are injected directly in the infarcted myocardium. This was the initial focus of research, which eventually was expanded to include cell culture, stem cell differentiation and scaffold development. These approaches were performed *in vitro* and then optimized for *in situ* delivery and implantation in the damaged myocardial area¹⁰.

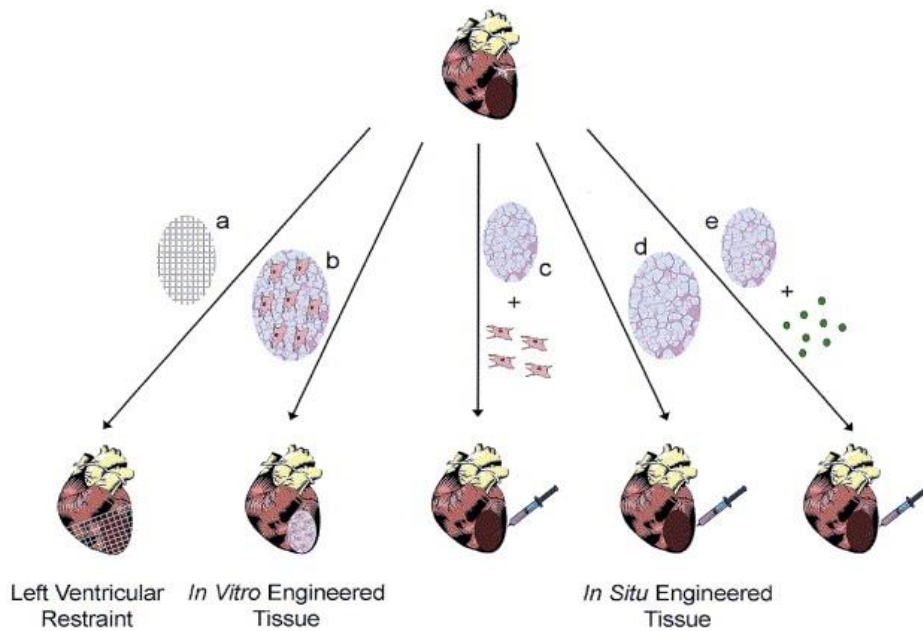


Figure 2.3 Three different treatment options for myocardial infarction. Polymer meshes sutured around the heart to (a) prevent further damage in the left ventricular (LV) (b) maintain the structure of LV. (c) Cultured cells on a biomaterial scaffold *in vitro* and implanted onto the epicardial surface (d) A biomaterial injected *in situ* (e) A scaffold injected *in situ* delivering cells, growth factors¹⁰.

A study conducted by Kelly et al. was the first to place a poly(propylene) Marlex mesh in the infarcted zone in the left ventricular (LV) to prevent the enlargement of tissue damage¹⁴. This approach was expanded further to demonstrate that the reason this patch could restrain the infarction was due to the blocking of metalloproteinases (MMPs) from being activated in the surrounding areas by serving as a gate around the infarcted zone of the myocardium. However, this approach did not change the increased volume of LV during infarction and scar tissue formation. Another polyester mesh has been fabricated and used by many research groups as a cardiac support device (CSD). In contrary from the previous mesh, this CSD can be placed to support both ventricles. This method has been shown to reduce the levels of MMPs, cardiac hypertrophy and LV volume but result in right ventricular (RV) dysfunction. Despite their relative benefits, the drawbacks of these techniques include surgery for implantation, lack of repair and regeneration of the damaged tissue, and failure to improve cardiac function¹⁰.

A possible better approach toward myocardial repair is the development of 3D biomimetic scaffolds suitable for cell attachment and survival. These scaffolds could be composed of various biodegradable materials; biological, synthetic or a combination of both.

2.3.1. 2D substrates

In the 1980's, significant research was done in understanding the role of the ECM proteins as cell seeding substrates that can be used in myocardial regeneration. Studies showed that cardiomyocytes could attach and proliferate on 2 dimensional (2D) substrates of collagen (type I, II, III, IV, and V), laminin and fibronectin. Adult

cardiomyocytes attachment was higher on laminin and collagen type IV, whereas neonatal cardiomyocytes attached better to fibronectin^{5,15,16}. Since ECM proteins are part of the native cardiac tissue, they are naturally biocompatible and suitable as cell seeding scaffolds needed for myocardial regeneration. This is shown by Bird et al. by comparing cardiomyocyte attachment on several 2D substrates. They cultured the cells on plates coated with 0.1% gelatin, 4% Fetal bovine serum (FBS), ECM (collagen I, IV), matrigel, laminin and poly-L-lysine. Also they used uncoated plates as control. The results showed that laminin and collagen IV provided the highest cell attachment and maintaining their structure for adult cardiomyocytes. The cells cultured on uncoated plates completely lost their sarcomere organization².

To further understand the role of ECM proteins in myocardial repair. Boateng et al. studied the cell attachment of cardiomyocytes and cardiac fibroblasts on RGD (Arg-Gly-Asp peptide¹⁷) and YIGSR (peptide in β -chain of laminin) synthetic peptides versus fibronectin and laminin where they naturally occur. The results showed that these synthetic peptides provided the same cell attachment as fibronectin and laminin. However they could not support sarcomere formation without the presence of the native ECM proteins¹⁸. Although these substrates provide cell survival and are biocompatible, they do not provide long term regeneration and can cause more damage with time. Also these scaffolds are 2D and do not provide the best support for cell morphology and contractile properties. Hence, 3D scaffolds might be a better option¹⁹.

2.3.2. 3D scaffolds

Collagen is among the main proteins used in scaffolds preparation. Given that

collagen is a native protein of the cardiac tissue, it is tested in developing various scaffolds for cell culture²⁰. Evans et al. created a 3D tubular scaffold composed of aligned collagen I fibers to study the development of cardiomyocytes. The cells aligned with the shape of the scaffold resembling neonatal phenotype and they expressed their contractile properties²¹. Collagen scaffold is proven to be a suitable environment for stem cell differentiation²⁰. However, the 3D scaffolds need to be developed further to become more suitable for *in vivo* transplantation. They need to not only provide survival conditions for the cells but also enhance their cardiac morphology and withstand their mechanical load. Therefore, another tissue engineering approach for creating suitable scaffolds for myocardial repair is being developed by incorporating nanofiber polymers.

Electrospun nano-fibers are being increasingly used to create scaffolds of biodegradable polymers, so as to mimic natural cardiac ECM features. This tissue engineering approach provides an essential opportunity of myocardial regeneration. Shin et al. cultured rat cardiomyocytes *in vitro* in a five layer scaffold composed of PCL nanofiber resembling an ECM structure. This scaffold was suspended on wire rings functioning as passive loads. The cells survived for 14 days and expressed cardiac properties. They started beating upon 3 days of seeding, gained synchronization and expressed cardiac proteins (α -myosin heavy chain, troponin I and connexin 43). However, the cardiomyocytes seeded in the innermost layers in this PCL mesh do not have the same access to fresh growth medium and might not have survived. Another limitation of this study is that the thickness of suspended wire ring is not appropriate for clinical applications⁷. In separate studies, it has been shown that the coating of PCL nanofibers with collagen can improve cell attachment and proliferation. A study

conducted by Zhang et al. compared two 3D scaffolds made of collagen and PCL nanofibers using two different techniques. The first was a composite of PCL fibers coated individually with collagen (Collagen-r-PCL) using a coaxial electrospun technique. The other scaffold was regular electrospun PCL fibers coated with collagen (collagen-coated PCL). Collagen-r-PCL showed a significant higher percentage of cell (fibroblasts) proliferation in *in vitro* culturing. However the limitation of this study is that the pore size of the Collagen-r-PCL scaffold might affect cell migration⁶.

The use of collagen in coating nanofiber composites (poly-lactide-co- ϵ -caprolactone) has resulted in increase of cell attachment and proliferation as well¹⁹. On the other hand, the uncoated nanofiber composites do not support cell attachment, according to Zong et al. They conducted a study using scaffolds composed of poly-L-lactide (PLLA), polyglycolide-based (PLGA) and a composite of PLLA, PLGA and polyethylene glycol (PEG). Rat cardiomyocytes cultured *in vitro* on these scaffolds expressed a better attachment and proliferation in the PLLA scaffold compared to the composite ones²². Many other polymers were used and tested *in vitro* and *in vivo* but they have encountered biological (necrosis) and mechanical issues (stiffness, mechanical unstable) mostly *in vivo*¹⁹. However, an improvement is seen when using aligned nanofibers in developing a scaffold. They provide better mechanical properties and better resemble the native cardiac ECM. Kai et al. cultured cardiomyocytes on non-aligned PCL nanofibers, aligned ones, random PCL/gelatin (PG) nanofibers and aligned ones. The study showed that aligned PG fibers favored cell attachment and their alignment. However, for long term repair of the myocardium the scaffold should be composed of the natural ECM molecules³. Hence, the 3D architecture of cardiomyocytes and the

surrounding ECM needs to be deeply understood.

2.3.3. *In vivo* studies

Many *in vivo* tests have been done to investigate the outcomes of various scaffolds in myocardial repair. Gelatin and alginate were used in scaffolds seeded with cardiomyocytes and implanted in the MI area. The studies showed that the cells survived and cardiac function was improved to a certain level¹⁰. However, the scaffolds should mimic the natural cardiac environment in porosity, pore size, alignment, texture, composition, etc. to provide the necessary support for cardiomyocytes and long term cardiac function improvement. Fibrin sealant (a mixture of blood derived adhesives mainly fibrin and thrombin,²³) is a hydrogel that has been injected directly in the infarcted area of the myocardium containing bone marrow cells and proved to increase vascular formation in the damaged tissue²⁴. Similar results were gained from injecting matrigel directly to the tissue¹⁹. Alginate gel is another injectable material that was tested *in vivo* and showed cardiac improvement²⁵. These materials help maintain shape of the myocardium, induce angiogenesis (neocapillary formation) and deliver cells or growth factors. Additional hydrogels that have similar properties in cardiac tissue repair are collagen, fibrinogen, gelatin, chitosan, hyaluronic acid to name a few¹⁹. Poly(ethylene) glycol (PEG) can be a suitable hydrogel for myocardium regeneration due to its viscoelastic properties and the fact that its physical and mechanical properties can be easily adopted during its polymerization. Dobner et al. performed an *in vivo* study using PEG hydrogel immediately following MI. This hydrogel provided myocardial remodeling initially but it did not provide long term repair^{26,27}.

Many other *in vivo* studies tested different hydrogels for their ability to help repair the infarcted myocardium. Zimmerman et al. cultured cardiomyocytes within a 3D gel composed of collagen type I, matrigel and growth medium of 1-4 mm thickness. This scaffold was transplanted in the rat heart and performed contractions up to 18 days by improving the cardiac function. However the drawback of this study is that this engineered heart tissue experienced a decrease in thickness due to probably necrosis being developed within the artificial tissue^{10,28}. The 3D scaffolds need to be developed further to become more suitable for *in vivo* transplantation. They need to not only provide survival conditions for the cells but also enhance their cardiac morphology and withstand their mechanical load.

Despite the wealth of information obtained from such studies, there is a significant dearth of data in the field of cardiac tissue engineering, specifically on the role of microenvironment on ECM protein synthesis and deposition by cardiomyocytes. How do the scaffold properties and characteristics influence matrix production by cardiomyocytes? What is the composition of the proteins deposited? Are any inflammatory and matrix-degrading enzymes released by cardiomyocytes? Obtaining information on these questions is not only crucial to understand cardiomyocyte biology *in vivo*, but also to develop tissue engineering and regenerative medicine based approaches to successfully integrate implanted cardiomyocytes with the native tissue.

2.4 Myocardial extracellular matrix

Cardiomyocytes compose 70-75% of the myocardium volume and are embedded

in a 3D ECM network of macromolecules. The macromolecules of this matrix are categorized into sarcomeric proteins, collagenous, glycoproteins, and GAGs. The sarcomeric proteins (actin, actinin, desmin, and filamin) are synthesized within the sarcomeres (basic unit of myocytes) that are linked to the subcellular structures via the help of other proteins such as fibronectin. Fibronectin is a glycoprotein similar to laminin and has been shown to improve cell attachment. The ECM proteins are essential in maintaining myocardial structure by providing mechanical support and tensile strength to the tissue^{14,15,29-31}. **Figure 2.4** shows the structure of the main ECM proteins, collagens, laminin and fibronectin present in the cardiac tissue.

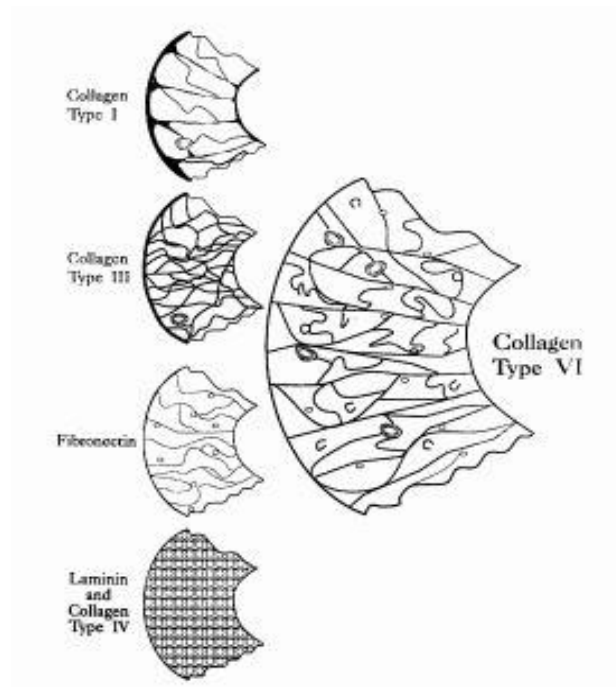


Figure 2.4 The architecture of the main proteins found in the cardiac tissue³¹.

Collagens

The major and most abundant protein in ECM is collagen which plays an important role in providing structure, support and tensile strength in the ECM and blood vessels. Collagen is presented in many different forms in the cardiac matrix where type I comprises 80% of the total collagen. Type III accounts for 12% and the remaining of the collagen volume constitutes of types IV, V, and VI. The collagens have a triple helix structure constructed with α -chains. The various combinations of the α -chains result in the different collagen types. For instance, collagen I is composed of two α -1 chains and one α -2 chain. The triple helix structure of collagen is held stable by the bonds that the hydroxylated amino acids of proline and lysine (hydroxyproline and hydroxylysine) form. Collagen I, III and V are fibrillar proteins forming collagenous aggregates to create collagen fibers. These proteins are found throughout the tissue providing structure and connecting cardiomyocytes together and to other tissue components such as fibroblasts and blood vessels. In the cardiac tissue collagen I and III is synthesized by fibroblasts whereas collagen IV is synthesized by cardiomyocytes. Collagen IV is found abundantly in the basement membrane of cardiomyocytes and is oriented perpendicular to the other collagen fibers resulting in a flexible matrix supporting network²⁹⁻³⁴.

Glycoproteins

Glycoproteins are a crucial part of the ECM. They regulate cell function, help in cell migration, attachment and proliferation. Fibronectin and laminin are two main glycoproteins that been shown to provide great attachment for cardiomyocytes^{14,15,32}.

Fibronectin is a major ECM molecule with a high molecular weight. As shown in **Figure 2.5 A**, fibronectin is a dimer composed of two polypeptide chains. This molecule contains multiple binding sites; it binds to integrins on cellular surfaces and other matrix molecules such as collagen and heparin. Additionally, fibronectin is present in the ECM in the form of fibrils which are formed on cell surfaces. Fibronectin has a role in cell organization and regulating cell function^{30,32,35}. It is found in abundance in the cardiac tissue in the endomysium³¹ and it is synthesized in the myocardium by fibroblasts following MI³⁴.

Another glycoprotein, fibrillin has similar properties with fibronectin. Fibrillin is the major component of microfibrils and can bind to integrins and other matrix macromolecules (proteoglycans). The main component of this glycoprotein is cystine and three isoforms are known up to date. An important role of fibrillin is that it mediates the assembly of elastic fibers³⁶.

Laminin is another major glycoprotein that is essential in ECM. Specifically, this protein is found in the basal laminae of the ECM associated with collagen IV. The molecule of laminin is built by the combination of three polypeptides (α , β and γ ; **Figure 2.5 B**) resulting in a large number of laminin isoforms. Additionally, laminin has the ability to self-assemble. Similar to fibronectin, this protein has many binding sites for cell surface molecules and other matrix components such as perlecan (heparan sulfated proteoglycan) and nidogen. Thus, laminin plays a role in cell organization as well^{31,32}.

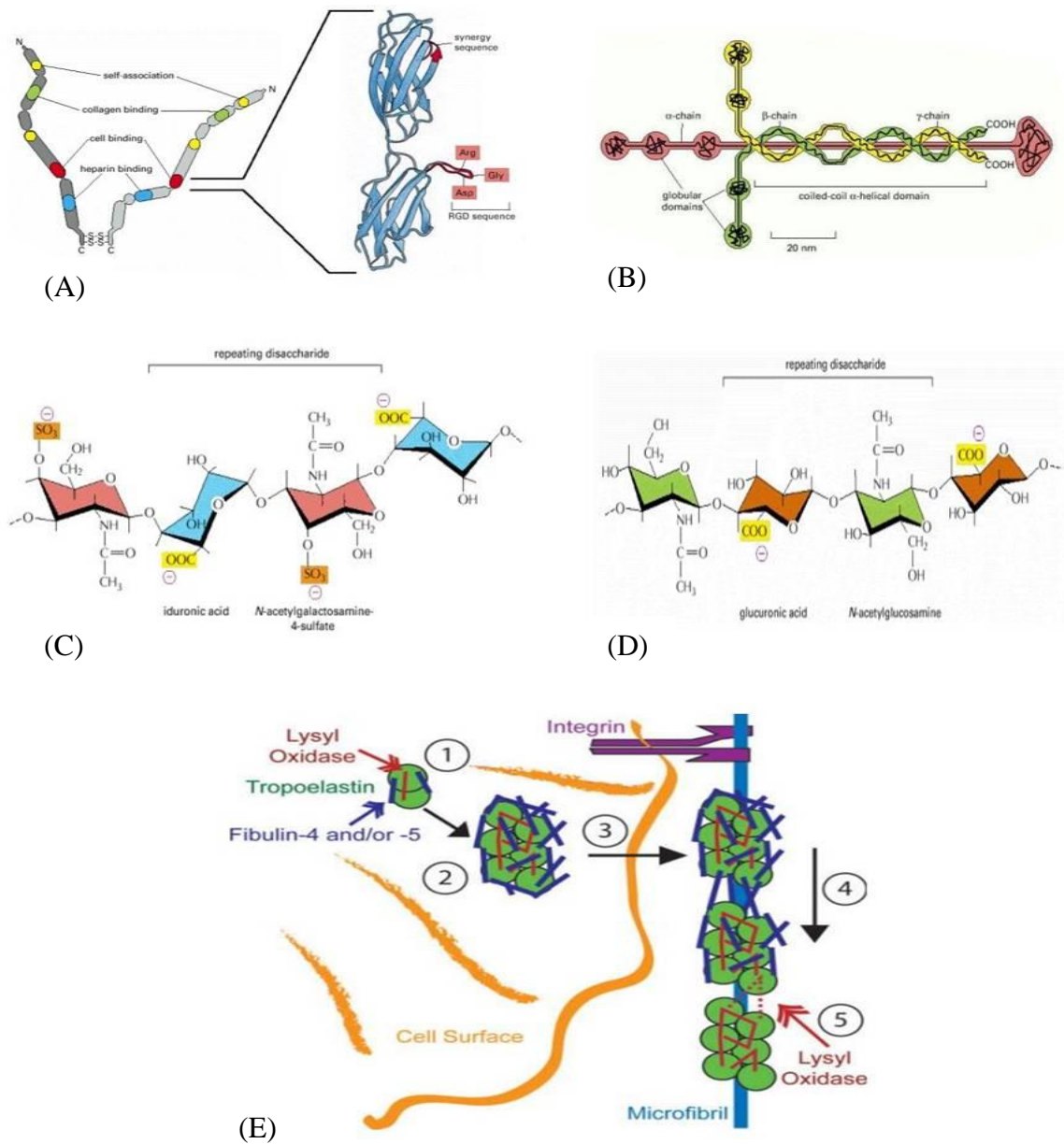


Figure 2.5 Structure of ECM molecules. (A) Fibronectin dimer; polypeptides linked by disulfide bonds. (B) Laminin composed of three different polypeptides chains linked by disulfide bonds. (C) Sulfated repeating disaccharide unit of GAGs. (D) Non-sulfated GAG disaccharide unit³². (E) Elastic fiber assembly: (1) tropoelastin cross-linked by LOX to form elastin polymer, (2) elastin polymer on the cell surface, (3) elastin polymers transferred to microfibrils through integrins, (4) larger elastin polymer formation, (5) Elastin polymer cross-linked by LOX to form final elastin protein³⁶.

Glycosaminoglycans

Glycosaminoglycans (GAGs) are anionic polysaccharides present in the ECM. They are hydrophilic chains with many disaccharide units. GAGs are divided in two main groups, sulfated GAGs (sGAGs) and non-sulfated GAGs, depending on whether one of the sugars is sulfated or not. GAGs are further categorized in four groups; hyaluronan, chondroitin sulfate, heparan sulfate, and keratan sulfate, based on the type of sugars, sulfate groups, and their bonding. **Figure 2.5 C** shows a structure comparison between sulfated and non-sulfated GAGs. The hyaluronan GAGs known as hyaluronic acid (HA) lack the sulfated sugar in its disaccharide unit as seen in **Figure 2.5 D**.

The hydrophilic property of GAGs causes them to expand in the form of gels and hence occupy a larger volume. This property is beneficial in resisting compressive forces in the myocardial ECM. Another property of GAGs is to covalently bond to other proteins forming a structure known as proteoglycans, except of HA. Furthermore, GAGs play an important role in regulating growth factor signaling activities or serving as co-receptors^{30,32,37}.

Elastin

Elastin is an essential ECM protein which confers elastic properties to blood vessels, among other functions. This protein is composed of cross-linked soluble monomers (tropoelastin) forming an insoluble protein mediated by the enzyme lysyl oxidase (LOX) (**Figure 2.5 E**). Elastin is assembled into fibers in the muscle tissue with the assistance of microfibrils, mainly fibrillin. Elastin is majorly synthesized during the

neonatal developing stages and a significant decrease is noticed in adult stages. This protein is very important in regulating blood flow due to the elasticity it provides in blood vessels bearing the mechanical pressure during cardiac cycle. It is shown that elastin regulates vascular smooth muscle cell proliferation and morphology in damaged cardiac tissue and prevents their deformation with the help of collagen. Hence, in cases of myocardial infarction the up regulation of elastin is needed to retain shape^{36, 38, 40}.

Matrix metalloproteinases and their inhibitors

Matrix metalloproteinases (MMPs) are extracellular proteolytic enzymes that degrade ECM proteins such as collagen, laminin and fibronectin. They are upregulated in the myocardium during an infarction. Their expression is increased after cardiomyocyte death to provide room for inflammatory cells. MMPs (1, 2, 3, 8, 9, and 13) degrade the ECM and the elevated collagen production by breaking down collagen cross-links. Furthermore, the synthesis of tissue inhibitors of metalloproteinases (TIMPs) is increased to protect the surrounding non-damaged tissue. These protease-specific TIMPs bind to the activated proteases during the inflammatory phase. However, during scar tissue formation MMP-9 and TIMPs are decreased drastically^{32, 34}.

CHAPTER III

MATERIALS AND METHODS

3.1 Scaffold preparation

3D hydrogel scaffolds

Six types of 3D hydrogel scaffolds with various compositions were prepared to evaluate the production and synthesis of ECM proteins by cardiomyocytes, as shown in Study I of **Table3.1** below. Rat-tail derived type-I collagen (3.84 mg/ml; BD Biosciences, Bedford, MA) was mixed with the appropriate volume of sterile 10× PBS, DI water and 1 N NaOH according to established protocols, to create collagen-I gels with concentrations of 1.2 mg/ml, 2 mg/ml and 3 mg/ml as detailed below.

To prepare 10 ml of 1.2 mg/ml collagen I, 3.125 ml of collagen I with initial concentration of 3.84 mg/ml was mixed with 1 ml 10× PBS, 71.9 µl of 1N NaOH and 5.8 ml DI water. To prepare 10 ml of 2 mg/ml collagen I, 5.2 ml of collagen I with initial concentration of 3.84 mg/ml was mixed with 1 ml 10× PBS, 119.6 µl of 1N NaOH and 3.68 ml DI water. To prepare 10 ml of 3 mg/ml collagen I, 7.8125 ml of collagen I with

initial concentration of 3.84 mg/ml was mixed with 1 ml 10× PBS, 179.7 µl of 1N NaOH and 1 ml DI water.

Collagen-I at 2 mg/ml concentration was mixed with 5% type-IV collagen (0.3 mg/ml; human-derived; Sigma-Aldrich, St. Louis, MO), 5% laminin (1 mg/ml; mouse-derived; Sigma-Aldrich) or 5% fibronectin (1 MG; Sigma-Aldrich) to prepare respective gels identified in **Table 3.1** as detailed below. To prepare collagen-I with 5% type-IV collagen, 5 ml of collagen-I 2 mg/ml was mixed with 833 µl collagen-IV. To prepare collagen-I with 5% laminin, 5 ml of collagen-I 2 mg/ml was mixed with 250 µl laminin. To prepare collagen-I with 5% fibronectin, 5 ml of collagen-I 2 mg/ml was mixed with 250 µl fibronectin.

Table 3.1 Scaffold compositions with respective notations.

	Composition	Notation
Study I	1.2 mg/ml collagen-I	CI-1.2
	2 mg/ml collagen-I	CI-2
	3 mg/ml collagen-I	CI-3
	2 mg/ml collagen-I + 5% collagen-IV	CI + CIV
	2 mg/ml collagen-I + 5% laminin	CI + LAM
	2 mg/ml collagen-I + 5% fibronectin	CI + FIB
Study II	Polycaprolactone fibers	PCL
	Collagen-I coated PCL fibers	PCL + CI
	Collagen-IV coated PCL fibers	PCL + CIV
	Laminin coated PCL fibers	PCL + LAM
	Fibronectin coated PCL fibers	PCL + FIB

Protein-coated PCL nanofiber scaffolds

Aligned polycaprolactone (PCL) nanofiber matrices (Nanofiber Solutions, Columbus, OH) were coated with ECM proteins such as collagen-I, collagen-IV, laminin and fibronectin. Non-coated fibers served as controls. Fiber matrices (fiber diameter ~ 700 nm; scaffold thickness ~ 20 microns) were placed within 24-well plates prior to coating with ECM proteins. Collagen-I and laminin solutions were prepared at 50 µg/ml concentration each in 0.02 N acetic acid and DI water, respectively. Collagen-IV and fibronectin were mixed with DI water each for a final concentration of 0.005% and 10 µg/ml, respectively. Collagen-I solution was added to the PCL nanofiber matrices (Study II in Table 3.1) and incubated at 37 °C for 1 h. After incubation, the solution was aspirated and wells were washed with DI water. Similarly, collagen-IV, laminin and fibronectin were added on the respective wells, left overnight at room temperature (RT), washed with 1× PBS, and stored.

3.2 Rat cardiomyocytes culture

Neonatal rat ventricular cardiomyocytes (R-CM) (4.0×10^6) were purchased from Lonza (Walkersville, MD) and cultured using the supplied medium (RCGM Bulletkit + 5-bromo-2'-deoxyuridine) in accordance with the provided protocol. The growth medium kit consisted of rat cardiomyocytes basal medium (RCBM), fetal bovine serum, horse serum, and gentamicin/amphotericin-B antibiotic, which were mixed and sterile-filtered. 5-bromo-2'-deoxyuridine (BrdU) stock solution was reconstituted in 1 ml of basal medium (40 mM) and sterile-filtered. The thawed cells were gently transferred from the cryovial into a 15 ml sterile tube, and 2 ml of pre-warmed R-CM media was added

immediately drop-wise onto the cells while rotating the tube. A 10 μ l aliquot of the cell suspension was mixed with an equal volume of Trypan Blue and the viable cells were counted using a hemocytometer.

Cell culture on 3D hydrogel scaffolds

R-CM were seeded within two different sets of scaffolds as explained in Table 1: collagen based hydrogels and protein-coated PCL nanofiber scaffolds. Cardiomyocytes were seeded within hydrogels at a density of ~ 26,000 cells/ well in 48-well culture plates (Greiner Bio One, Monroe, NC). The gel-laden plates were incubated at 37 °C for 30 min to allow for gel polymerization. Similarly, cells were seeded on protein-coated nanofiber plates at the same seeding density and allowed to attach. In both the cases, four hours after seeding, media was changed with fresh media. For every scaffold type listed in Table 1, at least n = 6 wells were cultured to perform each assay detailed in section 2.3. Cell cultures were performed for 21 days with media changed every three days. The pooled media was collected and stored at – 20 °C for biochemical assay analysis. At the end of 21 days, the cell matrices were detached from respective wells by incubating them with 1 \times trypsin-EDTA and processed for further analysis.

3.3 Live/Dead Viability/Cytotoxicity assay

The Live/Dead Viability/Cytotoxicity Kit was purchased from Life Technologies (Grand Island, NY) to perform the viability assay for R-CM survival rate. Initially, the 2 mM EthD-1 stock solution (Component B) was mixed with 1 \times PBS to create a 4 μ M EthD-1 solution. This solution was mixed with 4 mM calcein AM stock solution

(Component A) at a 2:1 ratio in accordance with the provided protocol. This EthD1 + calcein AM solution was vortexed to provide a thorough mixture. At the end of 21 days, the media was carefully removed from the R-CM cultures ($n = 3$ /hydrogel) and washed with $1\times$ PBS. Furthermore, they were incubated at 37°C , 5% CO_2 with the EthD-1 + calcein AM solution. The number of living cells was quantified to achieve the total cell count and survival rate of R-CM, using Zeiss Axiovert A1 fluorescence microscope.

3.4 Biochemical analysis

To characterize the ECM synthesized by the cardiomyocytes, several assays described in the following subsections were performed. These assay were conducted on cell matrix samples ($n = 3$ for each scaffold) and pooled media samples ($n = 3$ per case) from hydrogels and PCL nanofiber scaffolds ($n = 3$ for each case). At the end of the 21 day culture, the cell matrices were detached from respective wells by incubating them with Trypsin $1\times$ for 8-10 minutes. The cell suspensions were transferred to 2 ml microcentrifuge tubes and centrifuged gently at 2800-3000 rpm for 10-12 minutes. The supernatant was discarded and the pellet was resuspended in 100-300 μl $1\times$ PBS, depending on the assay, and stored in -20°C for further biochemical processing. The spent media was collected from each well over the 21 day culture period and stored at -20°C . These pooled media was aliquoted in 2 ml centrifuge tubes and centrifuged at 12000 rpm for 15 min. The supernatant was discarded and the pellet was homogeneously suspended in 100-300 μl $1\times$ PBS. The samples were stored in -20°C until further use.

BCA assay for total protein synthesis

The total amount of protein synthesized by R-CM was quantified using Pierce BCA Protein Assay kit (Thermo Scientific, Rockford, IL). The cell matrix and pooled media samples stored at -20 °C, were thawed and 25 µl of each sample were pipetted in a 96-well plate (Greiner Bio One, Monroe, NC). Standards of 25 µg/ml, 125 µg/ml, 250 µg/ml, 500 µg/ml, 750 µg/ml, 1000 µg/ml, 1500 µg/ml and 2000 µg/ml were prepared according to the provided protocol and pipetted in the 96-well plate. Additionally, 200 µl of BCA working solution (WR) was added to each well and mixed on a mechanical shaker for 30 sec. This BCA WR contains bicinchoninic acid (BCA) which contributes in the colorimetric capture of Cu^{1+} reduced from Cu^{2+} by the total protein present in the sample. Furthermore, the microplate was incubated at 37 °C for 30 min and cooled at RT measuring the absorbance at 562 nm on an EpochTM microplate spectrophotometer (Bio-Tek, Winooski, VT). The amount of protein measured was normalized to the total count of attached and survived cells.

sGAG assay

The sGAG Assay (Kamiya Biomedical Company, Seattle, WA) was used to quantify the amount of sulfated glycosaminoglycans deposited in the cell matrix and the pooled media under the various culture cases. A volume of 50 µl in duplicate of standards, blanks, controls, and samples was diluted with 50 µl of 8M Guanidine-HCl (GuHCl) and incubated for 15 min at RT. A diluent composed of 0.3% H_2SO_4 and 0.75% Triton X-100 (SAT) was added to each vial (50µl), mixed and incubated at RT for 15 min. Furthermore, 750 µl of Alcian Blue working solution was used in each vial to allow

the dye Alcian blue at a low pH, to bind to the sGAGs. The vials were incubated overnight at 4°C and the following day they were centrifuged at 12000g for 15 min. The supernatant was carefully removed using a syringe and the pellet was suspended in 500 µl DMSO solution and mixed on a mechanical shaker for 15 minutes. The centrifugation was repeated at 12000 g for 15 minutes and the supernatant was discarded. Finally, 500 µl of Gu-Prop (4M GuHCl + 33% 1-propanol + 0.25% Triton X-100) was used to dissolve the pellet. The samples were loaded on a 96-well plate and the absorbance was read at 620 nm using the microplate spectrophotometer. The data were normalized to the corresponding total cell counts.

Hyaluronic acid assay

The amount of hyaluronic acid (HA) synthesized in the cell matrix as well as released in the pooled media was quantified using HA-ELISA kit (Echelon, Salt Lake City, UT). This assay is based on the quantitative enzyme-linked immunoassay technique where HA binds to a specific enzyme-linked antibody. A volume of 100 µl samples and standards were pipetted in the provided 96-well incubation plate. The same amount of 1× HA diluent was pipetted serving as a zero HA control, whereas 150 µl of diluent was used as a blank control. The diluted HA Working Detector (50 µl) was added to all wells except the blank ones. The plate was gently mixed and incubated for an hour at 37 °C. After incubation, 100 µl solution was transferred from each well to corresponding wells in the pre-coated HA detection plate. The plate was incubated for 30 min at 4 °C. Following incubation, the plate was washed four times with 1× wash concentrate and it was inverted on absorbent paper to assure total removal of the wash concentrate. An

amount of 100 μ l of working enzyme was added to each well, mixed by gently tapping on the plate and incubated for 30 min at 37 °C. The washing procedure was repeated after incubation and 100 μ l of working substrate solution was added to each well. The detection plate was incubated in dark at RT for 15 min and the absorbance was measured at 405 nm every 15 min until the ratio between the zero HA control and 1600 ng/ml HA standard is higher than 3. This ratio indicates that incubation is complete and stop solution is added to each well. The data were normalized the respective cell counts.

Fastin elastin assay

The amount of tropoelastin produced in cell matrix and in pooled media, was quantified using Fastin Elastin Assay (Accurate Scientific Corp, Westbury, NY, USA). The samples stored at -20 °C were thawed and processed further to convert the insoluble elastin into soluble α -elastin form. Therefore the samples were heated at approximately 100 °C with 1 M oxalic acid for 1 h. The samples were transferred to 2 ml microcentrifuge tubes and an equal volume of elastin precipitating reagent was added. Additionally, a 1:1 ratio of elastin precipitating reagent was added in blanks and standards (12.5 μ l, 25 μ l, and 50 μ l). All samples and standards were run in duplicate and in accordance to the Fastin elastin assay protocol. Further, each tube was vortexed and for 15 min the reagent was allowed to help precipitate the elastin. The tubes were centrifuged at 10,000g for 10 min and the supernatant was discarded. The elastin precipitate was suspended in 1 ml dye reagent and homogeneously mixed. The dye reagent was left to bind to elastin for a period of 90 min on a mechanical shaker. Following this process, the tubes were centrifuged at 10,000g for 10 minutes and the supernatant was discarded. Dye

dissociation reagent (250 µl) was added to each tube and the pellet was dispersed by vortexing twice with a 10 minutes interval. Finally, the volume of each tube was transferred in a 96-well microplate and the absorbance was measured at 513 nm with the microplate spectrophotometer. The data were normalized to the total cell counts.

LOX functional activity

The activity of LOX in the cell matrix and pooled media was quantified with Amplex® Red Hydrogen Peroxide/Peroxidase assay kit (Molecular Probes, Eugene, OR). The thawed samples and prepared standards (0, 2, 4, 6, 8, and 10 µM) were pipetted (50 µl) in a 96-well microplate and the same volume of 50 µl of working solution (100 µM Amplex Red reagent, 1:2, 0.2 U/ml Horseradish peroxidase) was added to each well. The microplate was incubated in the dark at RT for 30 minutes. During the incubation period the working solution complex reacted with hydrogen peroxide (H₂O₂) released when LOX oxidatively deaminates alkyl monoamines and diamines. Following incubation, the absorbance of this enzyme activity was measured at 560 nm and final data were normalized according to the corresponding cell counts.

Quantification of MMP-2 and TIMP-1

The amount of MMP-2 and TIMP-1 released by R-CM in the spent collected media was determined using MMP-2 ELISA and TIMP-1 ELISA assay, respectively (Boster Biological Technology Co., Fremont, CA). The same provided protocol procedure was followed in both assays. Initially, the samples were diluted 2:1 with provided diluent buffer. Further, 100 µl of each sample was pipetted in the corresponding

MMP-2 and TIMP-1 specific antibody pre-coated 96-well plates. The respective standards were pipetted (100 μ l) in the respective plates as well. The microplates were covered and incubated at 37 °C for 90 min. Following incubation process, the content was removed and they were carefully blotted on absorbent paper without allowing the wells to dry. The incubation step was repeated with biotinylated anti-rat MMP-2 and biotinylated anti-rat TIMP-1 antibody working solutions (100 μ l per well) at 37 °C for an hour. The solution was discarded from each plate and the plates were washed three times with 1 \times PBS. The plates were incubated with 1 \times Avidin-Biotin-Peroxidase Complex (ABC) (100 μ l/well) for 30 min at RT followed by washing with 1 \times PBS five times to assure the total removal of any residues. TBM color developing agent was added, 90 μ l per well and the plates were incubated at 37 °C for 25-30 minutes before the reaction was terminated with 100 μ l of TMB stop solution in each well. The absorbance was determined at 450 nm and the sample data were normalized to the total cell count.

Quantification of MMP-9

MMP-9 ELISA assay (R&D Systems, Minneapolis, MN) was used to quantify the amount of this metalloproteinase that R-CM released in spent pooled media. This assay is based on the quantitative enzyme-linked immunoassay method where the MMP-9 binds to a specific monoclonal antibody and a specific enzyme-linked polyclonal antibody, the same technique followed by the previously presented MMP-2 and TIMP-1 assays. Initially, 50 μ l of diluent RD1-34 was pipetted to each well in the provided pre-coated 96-well plate. The same volume of standards and samples was added to the corresponding wells and the covered plate was incubated for two hours at RT. Further, the

wells were washed with wash buffer five times and 100 μ l of MMP-9 conjugate was added to each well. The plate was incubated at RT for another two hours and the washing step was repeated after incubation. Substrate solution was added, 100 μ l per well, and the plate was incubated in the dark at RT for a shorter time of 30 min. Finally, 100 μ l of stop solution was pipetted to each well and the absorbance was measured at 450 nm and 570 nm. The second values were subtracted from the first ones according to the protocol and the final data was normalized to the total R-CM count.

3.5 Immunofluorescence analysis

Immunofluorescence labeling was performed to qualitatively identify the presence of elastin, laminin, α -actinin, fibrillin and LOX in the cell matrix (**Table 3.2**). At the end of 21 days the culture wells were washed with 1 \times PBS and fixed in ice cold 4% paraformaldehyde (PFA) for 10 minutes (n = 2 per case). The PFA solution was removed and the cultures were washed with ice cold 1 \times PBS for 5 minutes. They were incubated with blocking agent [0.1% Triton-X, 5% goat serum (Sigma-Aldrich), 1X PBS] at RT for 20 minutes. Primary antibody solutions (1% antibody in 1X PBS, 5% goat serum, 0.1% Triton-X) were added directly to the respective cultures that were incubated overnight at 4 $^{\circ}$ C. The culture plates were kept on a mechanical shaker to assure complete antibody binding. Primary antibody solutions were removed and culture wells were washed 3 times with 1 \times PBS, 5 min per time. Secondary antibody (**Table 3.2**) solutions (0.4% antibody in 1 \times PBS, 5% goat serum, 0.1% Triton-X) were added and cultures were incubated for 20 min in dark at RT. Cultures were washed following the procedure mentioned above. At last, 4',6- diamino-2-phenylindole dihydrochloride (DAPI; Sigma-

Aldrich) was added to stain the cell nuclei. After removing the DAPI, 1X PBS was added to the cell cultures to preserve them while performing florescence imaging using the Zeiss Axiovert A1 florescence microscope.

Table 3.2 Summary of antibodies used for immunofluorescence analysis.

Primary antibody	Host	Clonality	Concentration (v/v)
Alpha-actinin	Rabbit	Polyclonal	1;100
Elastin	Rabbit	Polyclonal	1;100
LOX	Rabbit	Polyclonal	1;100
ELR	Rabbit	Polyclonal	1;100
Fibrillin	Rabbit	Polyclonal	1;100
Primary antibody	Host	Clonality	Concentration (v/v)
Goat anti-Rabbit	Goat	Polyclonal	1;250

3.6 Scanning electron microscopy

To visualize the structure of cardiomyocytes alignment along the nanofibers, the five cases of nanofiber coated scaffolds were imaged using a scanning electron microscopy (SEM). The nanofiber coated layers with attached cells were cut out and passed through a graded series of ethanol concentrations to dehydrate the cell matrix. The initial ethanol concentration used was 50% and it was increased by 10% up to the final concentration of 100%. In each dehydration step, the samples were soaked in ethanol for 10 minutes. Furthermore, samples were allowed to air dry for 30 minutes and were mounted on carbon tape and placed in Sputter machine (SPI sputter model 13131) where

they were coated in gold for 2 min. Samples were then imaged in the SEM (Amray 1820 using a IXRF 500 digital processor) using 10 KeV electron source at 500 and 1250 magnification.

3.7 Contractile properties of R-CM in PCL nanofiber scaffolds

The ability of R-CM to express their contractile properties was quantified in all five various PCL nanofiber scaffolds. Videos of contracting cells were recorded using the florescence microscope and Apowersoft Free Screen Recorder. The data was processed to quantify the number of beating cells, as well as their frequency across the five different cases.

3.8 Statistical analysis

All biochemical data obtained were analyzed using Sigmaplot and with the appropriate functions in MS Excel. Statistical significance values between experimental conditions were analyzed using Student's t-test and one-way ANOVA. Variance between data was considered significant at $p < 0.05$.

CHAPTER IV

RESULTS AND DISCUSSION

This chapter will present the data obtained from both sets of experiments. As described in Chapter III, neonatal rat cardiomyocytes were cultured *in vitro* for 21 days in six different 3D hydrogel scaffolds (CI-1.2, CI-2, CI-3, CI + CIV, CI + Lam, CI + Fib), as well as in five different aligned PCL nanofibers coated with the ECM proteins (collagen I, collagen IV, laminin, fibronectin) including an uncoated PCL nanofiber plate as control. Cell survival rate and ECM synthesis were analyzed both quantitatively and qualitatively and are presented in the following sections.

4.1 Hydrogel scaffolds

4.1.1 Live/Dead Viability/Cytotoxicity assay

The viability assay was performed at the end of the 21 day culture period of the rat cardiomyocytes. The data for live cell counts are shown in **Figure 4.1**. Among the three concentrations of collagen I tested, 2 mg/ml hydrogel provided the highest survival rate

(91±4%), compared to the other two cases. Collagen hydrogels support most of the cardiomyocytes to survive and allow them to form a 3D network within the hydrogels [41]. Increasing collagen I concentration to 3 mg/ml significantly decreased cardiomyocyte survival rate (72%; $p < 0.01$ for 3 mg/ml vs. 2 mg/ml; $p < 0.01$ for 3 mg/ml vs. 1 mg/ml). However, no statistically significant difference in cell survival was noticed between 2 mg/ml and 1 mg/ml cases. Likewise, a low cell survival rate (77±4%) was seen in 2 mg/ml collagen I scaffolds, mixed with collagen IV. While coating 2mg/ml collagen I scaffolds with fibronectin promoted significantly higher cell survival rate (88±4%) compared to collagen-IV and laminin-coated scaffolds ($p < 0.01$ in both the cases), no significant differences were noted between collagen-IV and laminin coated cases. Similar effects of fibronectin and laminin 2D substrates on embryonic and neonatal cardiomyocyte survival, was reported by Evans et al. Fibronectin 2D substrates, collagen I 2D substrates and collagen 3D scaffolds provided over 85% cell survival rate, whereas laminin allowed for approximately 55% cell survival²¹. Taken together, these results suggest that:

- ⤴ collagen concentration plays an important role in cardiomyocyte survival, with higher concentration resulting in more stiffness and less porosity, thereby decreasing cell survival. An increase in collagen concentration accounts for a higher mechanical stiffness (G^*)⁴², and
- ⤴ Coating 2 mg/ml collagen scaffolds with ECM proteins may not benefit cardiomyocyte survival beyond that offered by un-coated scaffold (e.g., fibronectin), and in fact might be detrimental to cell survival (e.g., laminin, collagen-IV). However, the reasons for this behavior are not clear at this stage and

needs further investigation.

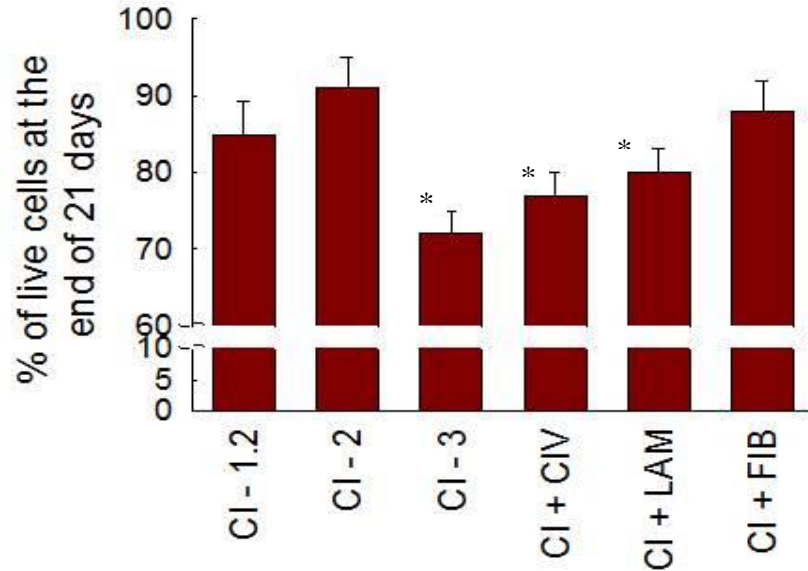


Figure 4.1 The percentage survival rate of rat cardiomyocytes at the end of 21 day culture, obtained from Live/Dead Viability assay (n=2). Data was shown as mean \pm standard error.

As shown in previous studies, collagen hydrogels support the majority of seeded cardiomyocytes to survive and allow them to form a 3D network within the gels⁴¹. However a higher concentration gel causes a decrease in cell survival⁴². This is due to an increase in collagen concentration accounting for a higher mechanical stiffness (G^*)⁴³.

4.1.2 Biochemical analysis

Total protein synthesis and deposition

The total amount of protein synthesized by cardiomyocytes is divided into two parts: that deposited within the cell layers in the matrix, and that released in the pooled

media (**Figure 4.2 A**). The results obtained from the BCA assay, were normalized to the total cell count obtained from the viability assay. Data suggests that among the three different collagen concentrations tested, cardiomyocytes cultured within CI-2 hydrogel released the lowest amount of protein in pooled media ($p < 0.001$ vs. other two cases). However, cells within this scaffold promoted significantly higher amounts of protein deposition within cell matrix compared to the other two cases ($p < 0.001$). Interestingly, changing the collagen concentration to 1 or 3 mg/ml, significantly increased the protein content collected in the pooled media (1.68- and 1.54 –fold respectively, compared to CI-2). However, these increases in protein release in pooled media could not be translated into gains in matrix deposition. It was noticed that altering the hydrogel stiffness significantly decreased the amount of protein deposited in the cell matrix (**Fig. 4.2 A**). Mixing the CI-2 scaffolds with collagen-IV or laminin significantly increased the protein synthesis and release into pooled media ($p < 0.001$ in both the cases compared to CI-2), while fibronectin coating did not elicit significant changes ($p > 0.1$ vs. CI-2). However, adding laminin significantly reduced protein deposition within cell matrix ($p < 0.01$ vs. CI-2) to levels noticed in CI-1.2 or CI-3 scaffolds. The protein deposition into matrix within fibronectin-mixed scaffolds was the lowest of all the cases ($p < 0.01$ vs. all the other cases), while that in collagen-IV mixed scaffolds was comparable to that in CI-2. Taken together, results suggest that collagen concentration (and therefore stiffness) and protein addition stimulate varied levels of protein synthesis from rat cardiomyocytes, with CI-3 and CI+CIIV offering the optimal conditions for higher amounts of protein synthesis.

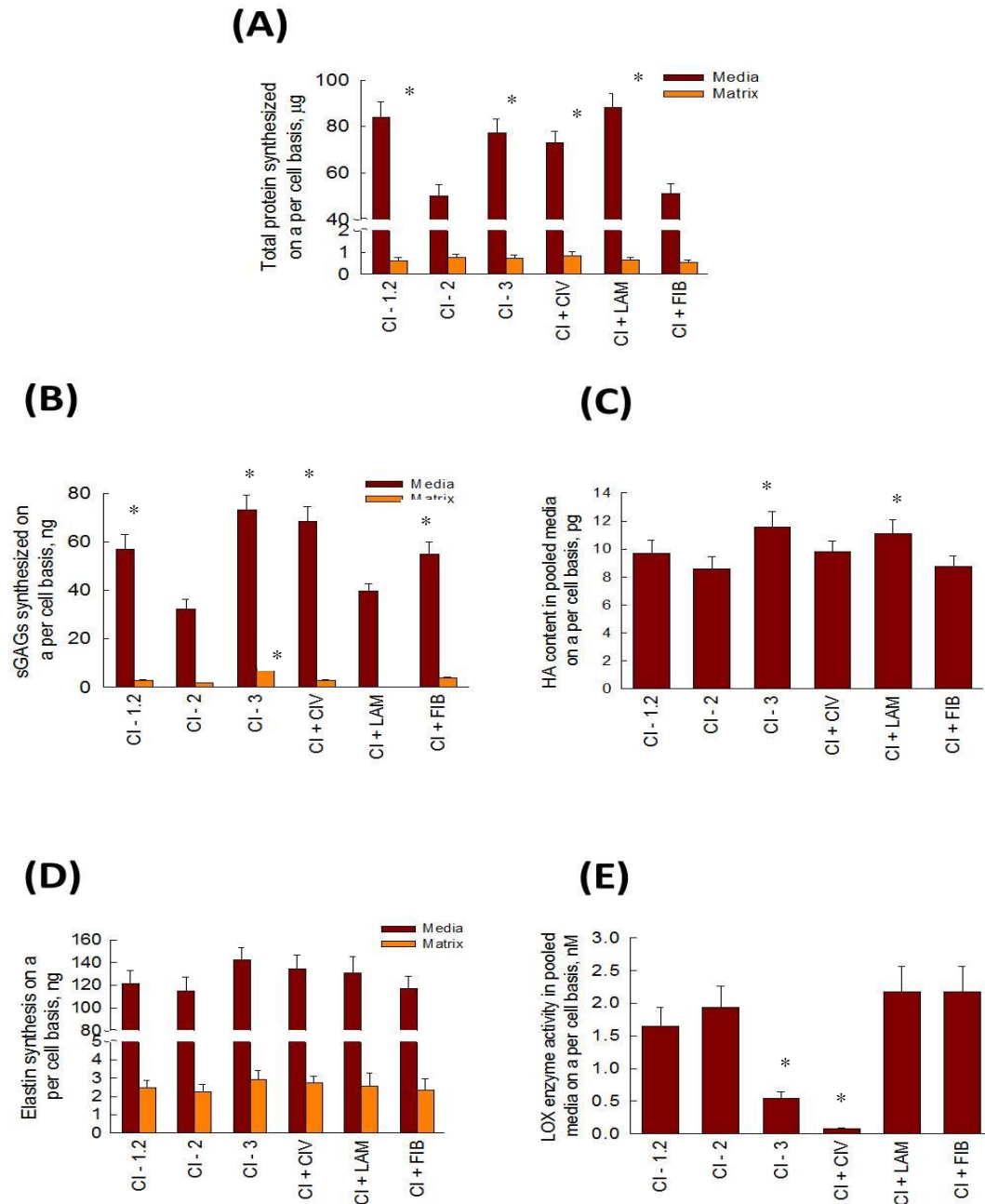


Figure 4.2 Protein syntheses by rat cardiomyocytes at the end of 21 day culture (n=3). Data was shown as mean \pm standard error. **(A)** Total protein synthesized in cell matrix and released in pooled media on a per cell basis, obtained from BCA protein assay. **(B)** Amount of sGAGs synthesized in cell matrix and released in pooled media on a per cell basis, obtained from sGAG assay. **(C)** HA content released in pooled media on a per cell basis, obtained by HA ELISA assay. **(D)** Elastin synthesized in cell matrix and released in pooled media on a per cell basis, obtained by Fastin Elastin assay. **(E)** LOX content released in pooled media on a per cell basis, obtained by Amplex® Red Hydrogen Peroxide/Peroxidase assay.

Sulfated-glycosaminoglycan (sGAG) release and deposition

The content of sGAGs produced by rat cardiomyocytes varied through the six cases of hydrogel scaffolds (**Figure 4.2 B**). The data from the sGAG assay were normalized to the total cell count within respective cases. It was noted that collagen at 3 mg/ml was the most conducive scaffold for sGAG synthesis and release into pooled medium as well as deposition into matrix layers, followed by 1.2 mg/ml and 2 mg/ml, respectively ($p < 0.01$ for CI-3 vs. CI-1.2 and CI-3 vs. CI-2; $p < 0.01$ for CI-1.2 vs. CI-2). Within laminin-coated CI-2 scaffolds, sGAG release into pooled medium remained unaffected compared to CI-2 cases ($p > 0.1$), but no quantifiable sGAG presence was noted within cell layers. Within fibronectin and collagen-IV mixed scaffolds, elevated levels of sGAG was quantified in both pooled media and matrix, compared to CI-2 gels ($p < 0.01$ vs. CI-2). Taken together, data suggests that CI-3 and CI+CIV scaffolds provide optimal environment for sGAG synthesis, release and deposition in the cell layers.

Hyaluronic acid synthesis and release

The HA-ELISA assay was used to detect the content of HA protein in cell matrix and in pooled media (**Figure 4.2 C**), and normalized to cell counts at the end of the 21 day culture. Among the various collagen concentrations tested, CI-3 appeared to offer a better substrate for HA synthesis and release in pooled media ($p < 0.01$ for CI-3 vs. CI-1.2 and CI-3 vs. CI-2). Quantifiable HA amounts in cell matrix were not detected in all the cases. Similarly, laminin-coating offered a better substrate for HA release compared to fibronectin ($p < 0.01$), although it was not significantly higher than that in collagen-IV mixed substrates. Nevertheless, dramatic changes in HA synthesis or release was not

noted with changing concentration or protein-coating.

Elastin synthesis, deposition and crosslinking

The results from the Fastin elastin assay are presented in **Figure 4.2 D**, with the amount of tropoelastin (in pooled media) and matrix elastin normalized to the total cell count. Among all the scaffolds tested, CI-3 followed by CI+CIV, appeared to offer better conditions for elastin production and deposition. The lowest content of tropoelastin in both cell matrix and pooled media was assessed in CI-2 hydrogel. These results were in broad agreement with trends in the sGAGs and total protein synthesis by rat cardiomyocytes cultured within CI-3 and CI+CIV scaffolds.

Lysyl oxidase enzyme activity within pooled media

LOX activity was measured for each case and normalized to the respective cell count (**Figure 4.2 E**). LOX activity in the cell matrix was too low to be accurately quantified. The cells cultured in CI + Lam and CI + FIB expressed similar amounts of LOX activity in pooled media, but not significantly higher than that in CI-2. However, a dramatic decrease in LOX activity was seen in CI + CIV scaffolds. Although no significant differences in LOX activity were noted between CI-1.2 and CI-2 cases, it was significantly lower in CI-3 scaffolds ($p < 0.01$ for CI-3 vs. CI-1.2 and CI-3 vs. CI-2).

Quantification of MMPs-2, 9 and TIMP release

The release of MMP-2 in pooled media was quantified and normalized on a per cell basis (**Figure 4.3 A**). The lowest MMP-2 release was noted in CI- 1.2 hydrogel, and

it progressively increased with increasing collagen concentration ($p < 0.01$ for CI-3 vs. CI-1.2 and CI-3 vs. CI-2). Mixing CI-2 scaffolds with collagen IV further increased MMP-2 release, compared to pure collagen scaffolds. The presence of fibronectin and laminin appeared to further increase MMP production, compared to adding collagen IV. Among all the cases tested, the presence of laminin seemed to elicit the highest MMP-2 release. It was interesting to note that the presence of ECM proteins such as laminin, fibronectin and collagen IV promotes higher release of MMP-2 by rat cardiomyocytes.

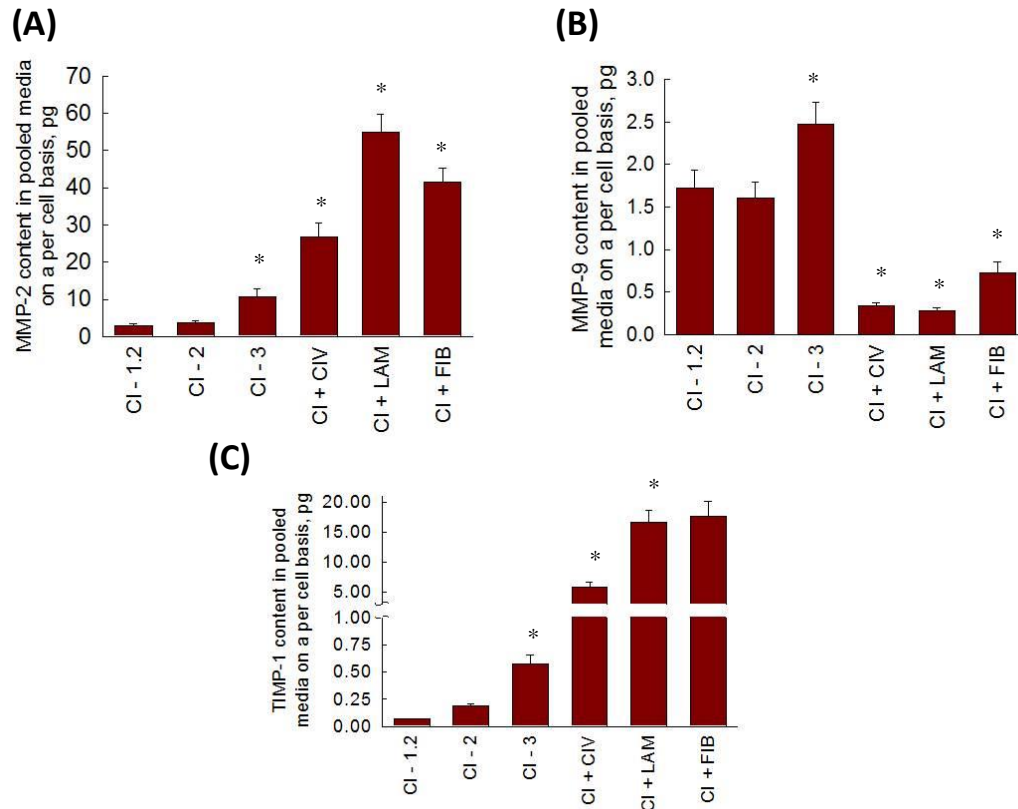


Figure 4.3 Quantification of MMPs and TIMP expressed by rat cardiomyocytes at the end of 21 day culture (n=3). Data was shown as mean \pm standard error. **(A)** MMP-2 content in pooled media on a per cell basis obtained by MMP-2 assay. **(B)** MMP-9 released in pooled media on a per cell basis obtained by MMP-9 assay. **(C)** TIMP-1 content in pooled media on a per cell basis obtained by TIMP-1 assay.

MMP-9 release by rat cardiomyocytes into pooled media is (**Figure 4.3 B**) exhibited different trends compared to MMP-2 release. Collagen-I at 3 mg/ml concentration promoted significantly higher amounts of MMP-9 release, compared to 1.2 and 2 mg/ml concentrations ($p < 0.01$ for CI-3 vs. CI-2 and CI-3 vs. CI-1.2). In contrast to the trends noted for MMP-2 release, addition of collagen-IV, or laminin or fibronectin drastically reduced MMP-9 release ($p < 0.01$). Among these 3 proteins, fibronectin appeared to elicit higher MMP-9 production and release by rat cardiomyocytes.

TIMP-1 synthesis and release by rat cardiomyocytes into pooled media was normalized to the respective cell count (**Figure 4.3 C**). Trends in TIMP-1 release were in contrast to that observed for MMP-9, but similar to those of MMP-2 release. The amount of TIMP-1 released was in positive correlation to the concentration of collagen I. Changing the composition of CI-2 hydrogel by adding 5% collagen IV significantly increased the amount of protease released in pooled media. The addition of 5% laminin or 5% fibronectin, to CI-2 scaffolds, furthered this increase in TIMP-1 production.

4.1.3 Immunofluorescence analysis

The qualitative data obtained from immunofluorescence analysis is presented in **Figures 4.4** and **4.5**. The immunofluorescence labeling confirmed the protein synthesis trends noted in different cultures from quantitative ELISA assays for elastin and LOX. Immunofluorescence staining was also performed for fibrillin, elastin-laminin receptor (ELR), and α -actinin proteins, which confirmed the elastin assembly process in respective cases.

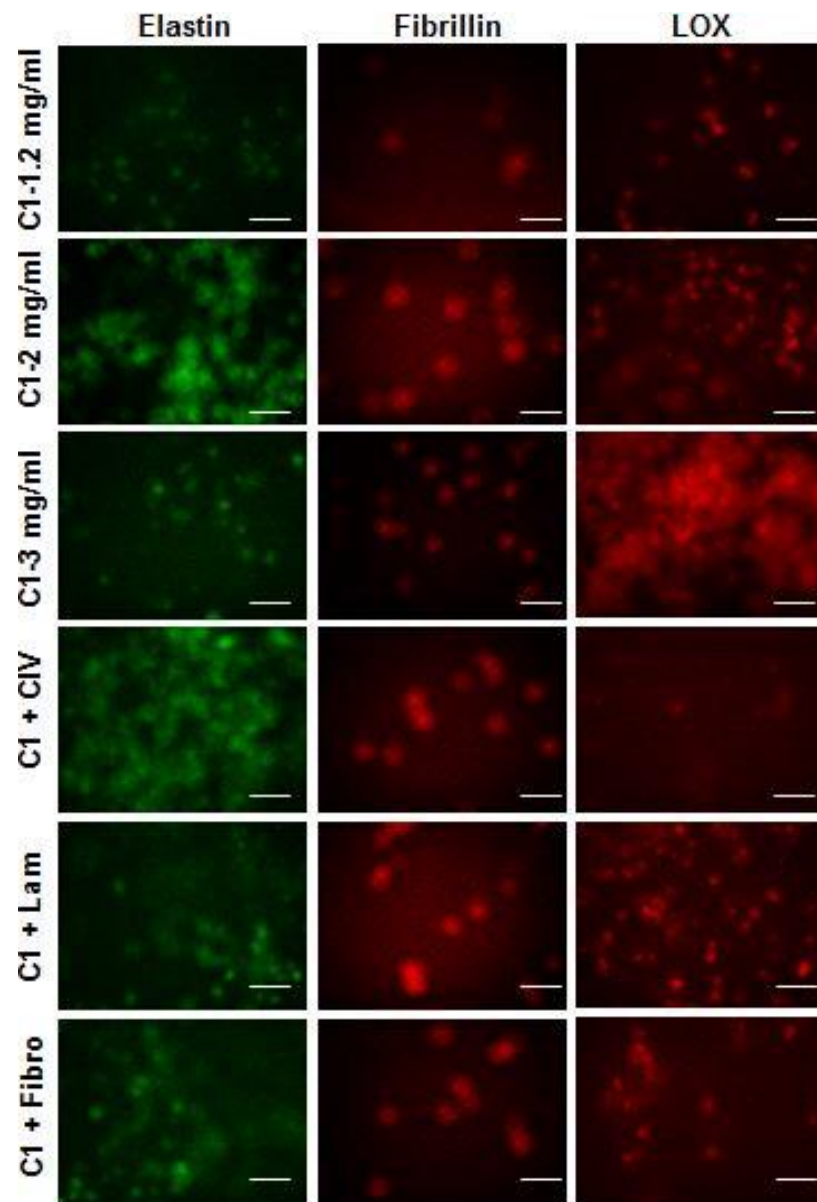


Figure 4.4 Immunofluorescence images showing staining of rat cardiomyocytes at day 21 for Elastin, Fibrillin and LOX. (n=2; 40x magnification; scale bar = 40 μ m).

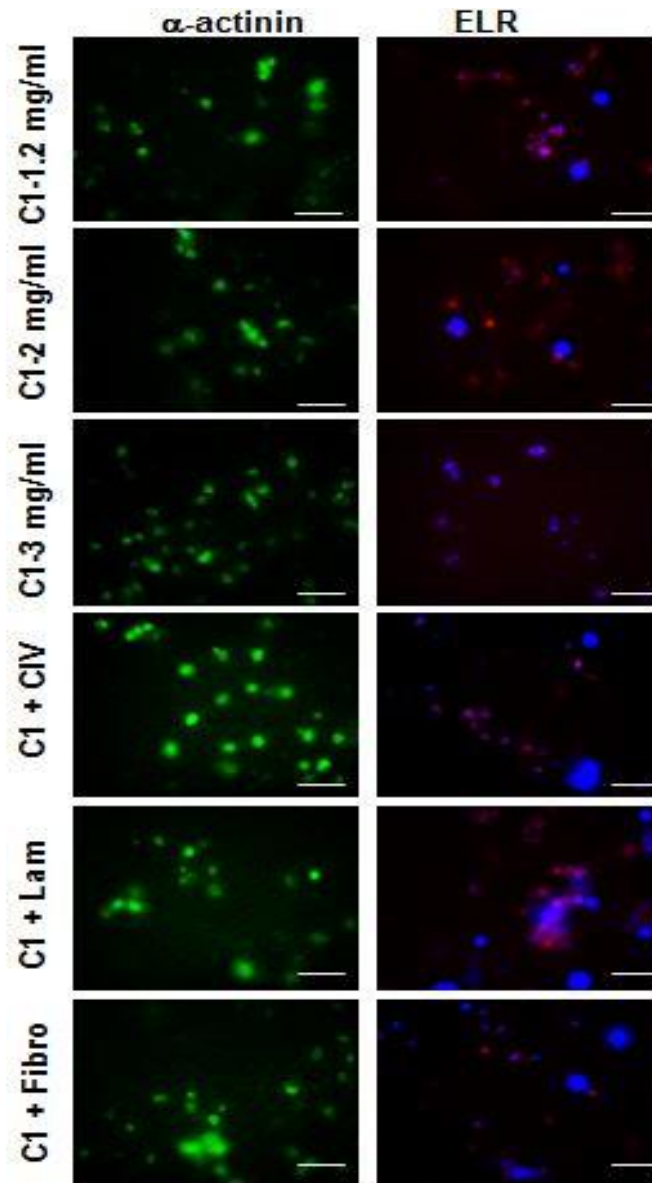


Figure 4.5 Immunofluorescence images showing the α -Actinin and ELR staining of rat cardiomyocytes at day 21. Nuclei are DAPI stained blue. (n=2; 40x magnification; scale bar = 40 μ m)

4.2 PCL nanofiber coated scaffolds

4.2.1 Live/Dead Viability/Cytotoxicity assay

The percentage of survived cells in each type of nanofiber scaffold gathered from the viability assay is shown in **Figure 4.6**. Cardiomyocytes survival on uncoated PCL nanofiber plates was significantly lower compared to the protein-coated fiber scaffolds ($p < 0.01$ for PCL vs. other scaffolds). Kai et al. also reported that cardiomyocytes expressed higher survival rate in gelatin coated PCL aligned nanofibers compared to uncoated ones³. Compared to fibronectin, other proteins (laminin, collagen IV and collagen I) enhanced cell survival ($p < 0.01$ for PCL+FIB vs. other three proteins).

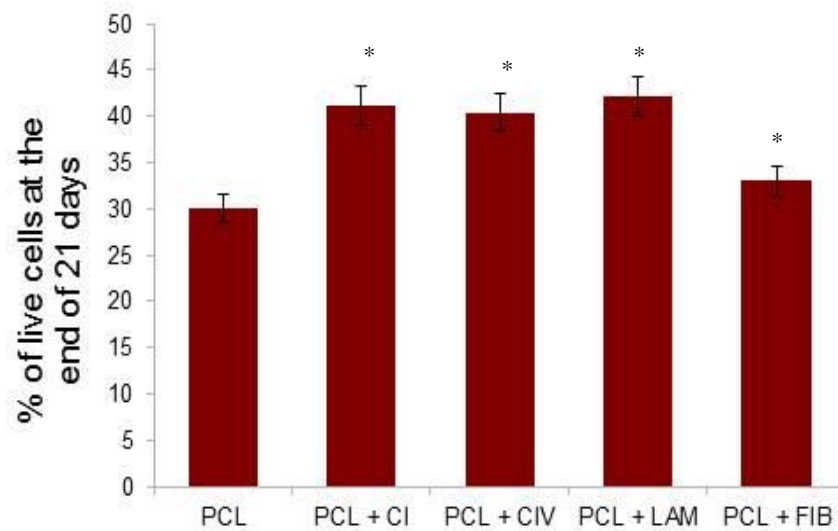


Figure 4.6 The percentage survival rate of rat cardiomyocytes at the end of 21 day culture, obtained from Live/Dead Viability assay (n=2). Data was shown as mean \pm standard error.

4.2.2 Biochemical analyses

The total amount of protein synthesized by rat cardiomyocytes was quantified and normalized on a per cell basis as shown in **Figure 4.7 A & B**. The cells cultured on PCL + FIB scaffolds synthesized higher amount of protein compared to fibers coated with collagen I, collagen IV, or laminin, in both cell matrix and pooled media. Within cell matrix, the total protein content in collagen-IV coated fibers was the lowest ($p < 0.001$), while that in fibronectin-coated fiber scaffolds was the highest ($p < 0.001$), compared to other scaffolds.

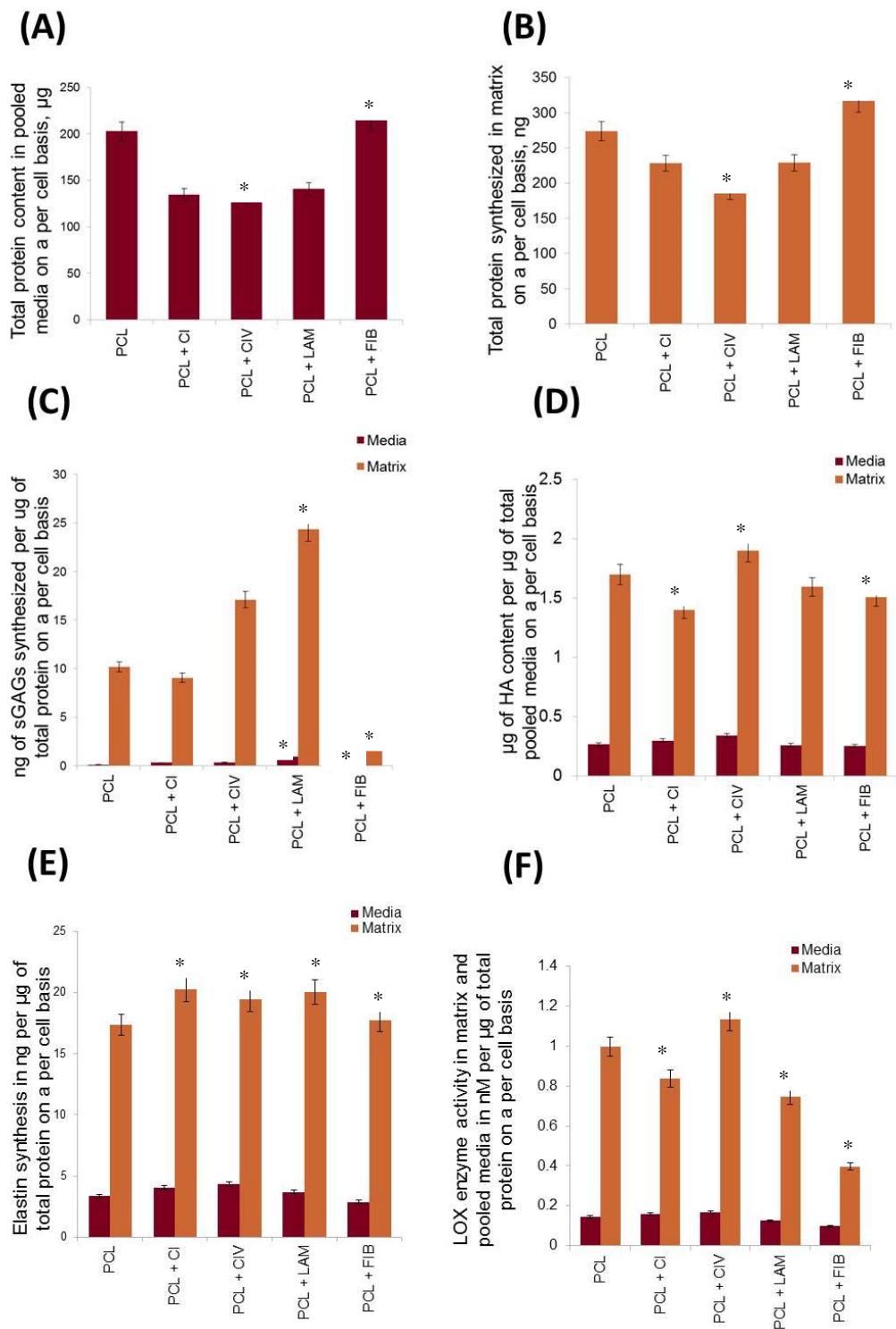


Figure 4.7 Proteins expressed by rat cardiomyocytes at the end of 21 day culture (n=2). Data was shown as mean \pm standard error. **(A)** Total protein released in pooled media on a per cell basis, obtained from BCA protein assay. **(B)** Total protein synthesized in cell

matrix on a per cell basis, obtained from BCA protein assay. **(C)** sGAGs synthesized in cell matrix and released in pooled media normalized to the total protein amount on a per cell basis, obtained from sGAG assay. **(D)** HA content in cell matrix and released in pooled media normalized to the total protein on a per cell basis, obtained by HA ELISA assay. **(E)** Elastin synthesized in cell matrix and released in pooled media normalized to the total protein amount on a per cell basis, obtained by Fastin Elastin assay. **(F)** LOX content in cell matrix and released in pooled media normalized to the total protein on a per cell basis, obtained by Amplex® Red Hydrogen Peroxide/Peroxidase assay.

Figure 4.7 C shows the results from sGAG assay, normalized per μg of total protein synthesized in respective cases, and further normalized to the total cell count. Compared to uncoated fibers, coating with collagen IV or laminin significantly improved sGAGs synthesis released into pooled media ($p < 0.001$ vs. uncoated PCL fibers). However, sGAG deposition within cell matrix was significant only within laminin coated scaffolds. Compared to all the cases tested, laminin coating drastically increased the synthesis of sGAGs in both cell matrix and pooled media ($p < 0.001$ for laminin vs. all other cases). Contrarily, for reasons unclear at this stage, the presence of fibronectin on the PCL nanofibers dramatically inhibited the synthesis, release and deposition of sGAGs in the cell matrix and in the pooled media, compared to all the other cases.

HA synthesis was quantified in cell matrix and pooled media and normalized to the total protein content within respective cases, and further to cell count, as shown in **Figure 4.7 D**. Collagen IV-coated PCL cultures expressed the highest amount of HA in cell matrix and pooled media, compared to controls and all the other cases. The lowest HA content was observed in collagen I- and fibronectin- coated fiber scaffolds, lower than that compared to controls ($p < 0.01$ vs. controls). However, no significant differences between controls and laminin-coated PCL cultures were noted.

The amount of tropoelastin synthesized by rat cardiomyocytes within each type of scaffold was normalized to total protein content and further to the cell count within respective cases as shown in **Figure 4.7 E**. Except fibronectin-coated scaffolds where significant decrease in both tropoelastin and matrix elastin was noted ($p < 0.01$ vs. controls), significantly higher tropoelastin and matrix elastin amounts were observed in all the other three protein coated (collagen I, collagen IV, and laminin) scaffolds. The LOX enzyme activity was normalized on a per cell basis and is shown in **Figure 4.7 F**. LOX enzyme activity was higher in collagen IV-coated PCL nanofibers compared to controls ($p < 0.01$). Within the other three protein coated scaffolds, cells deposited a significantly lower amount of LOX in the cell matrix and in the pooled media ($p < 0.01$ vs. controls). Among all the cases, fibronectin presence seemed to elicit the lowest LOX enzyme activity in both cell matrix and pooled media

Quantification of MMPs-2, 9

The MMP-2 production was normalized to the total cell count and the total protein content and the data is shown in **Figure 4.8 A**. The presence of collagen I or fibronectin on the PCL nanofiber scaffolds decreased the content of MMP-2 collected in pooled media compared to uncoated PCL nanofiber scaffold. However, collagen IV and laminin increased the content of MMP-2 released in pooled media. Among these proteins, collagen I inhibited the amount of MMP-2 in pooled media the most, whereas collagen IV promoted its release the most.

A different trend is noticed in the production of MMP-9 as seen in **Figure 4.8 B**.

In all the test cases, where PCL fibers were coated with proteins, significant increase in MMP-9 release was noted compared to controls ($p < 0.01$ vs. controls). Laminin-coated PCL scaffolds promoted the highest MMP-9 release in pooled media.

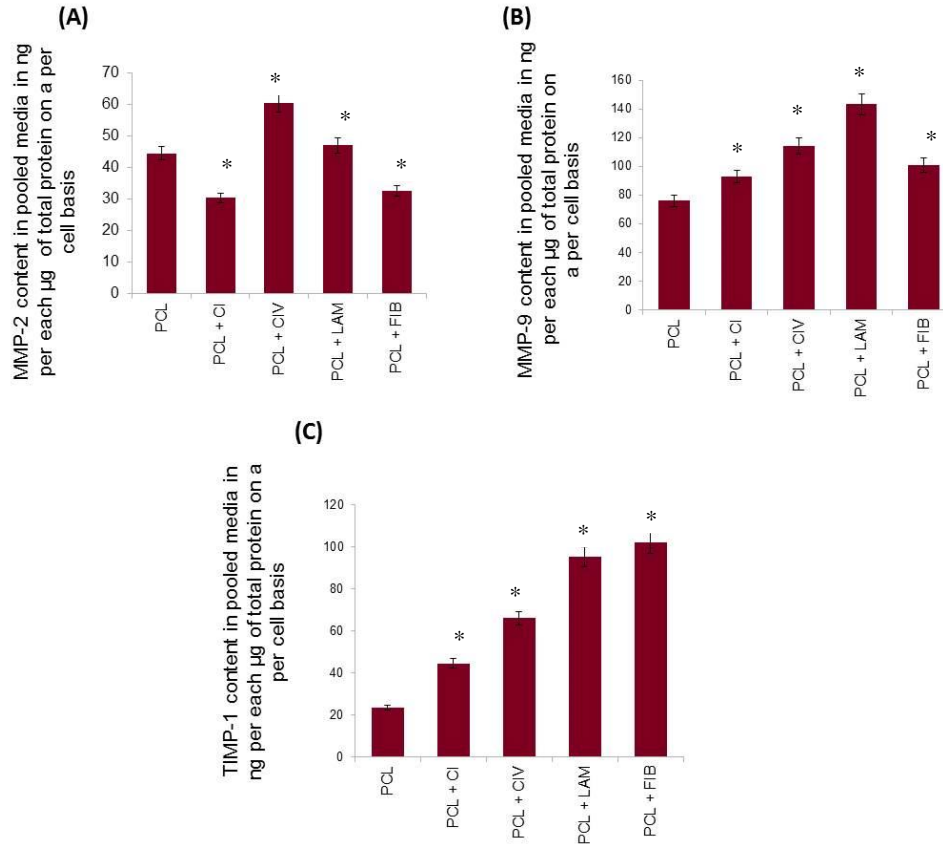


Figure 4.8 Quantification of MMPs and TIMP expressed by rat cardiomyocytes at the end of 21 day culture (n=3). Data was shown as mean \pm standard error. **(A)** MMP-2 content in pooled media on a per cell basis obtained by MMP-2 assay. **(B)** MMP-9 released in pooled media on a per cell basis obtained by MMP-9 assay. **(C)** TIMP-1 content in pooled media on a per cell basis obtained by TIMP-1 assay.

Quantification of TIMP-1

The results of TIMP-1 production are presented in **Figure 4.8 C**. A trend similar to MMP-9 production was observed in this case. Uncoated PCL nanofibers resulted in the lowest TIMP-1 content released in pooled media, whereas the ECM proteins expressed

drastically higher TIMP-1 content. The order of this increase was as follows, collagen I, collagen IV, laminin and fibronectin accounting for the highest TIMP-1 content.

4.2.3 Immunofluorescence analysis

Immunohistochemistry data showed positive staining for α -actinin, ELR, Elastin, LOX, and Fibrillin proteins, and the data is shown in **Figure 4.9** and **4.10**.

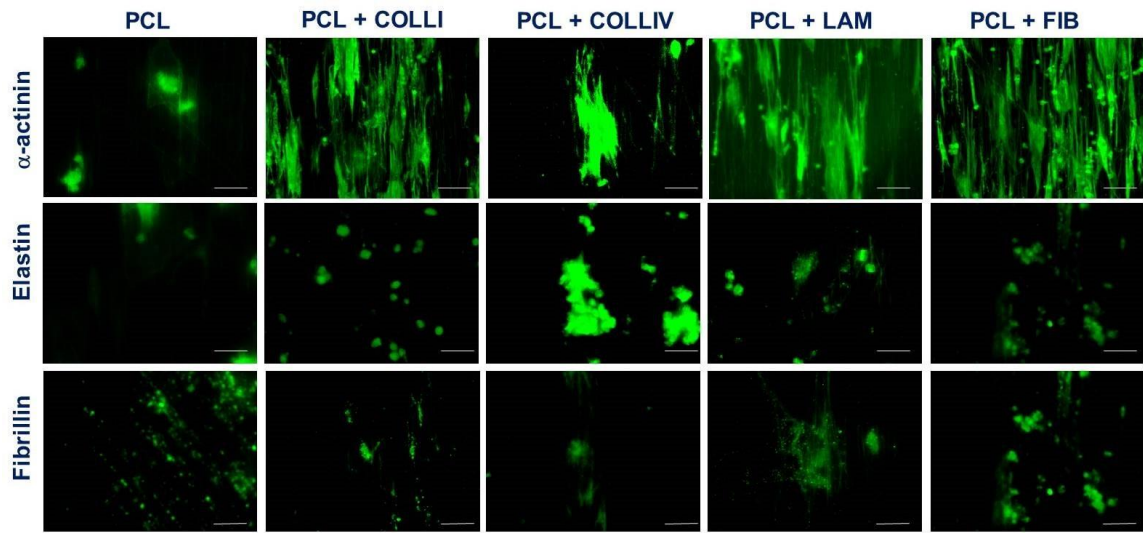


Figure 4.9 Immunofluorescence images showing staining of rat cardiomyocytes at day 21 for Fibrillin, Elastin, and α -actinin. (n=2; 40x magnification; scale bar = 40 μ m)

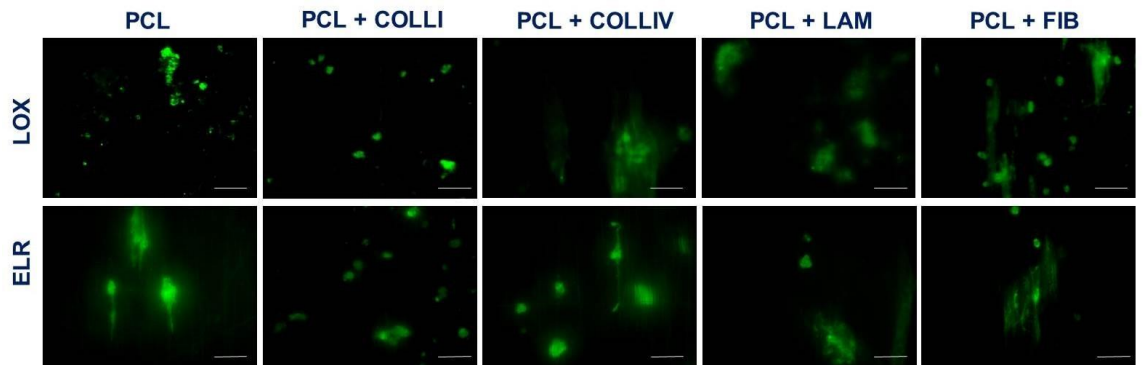


Figure 4.10 Immunofluorescence images showing staining of rat cardiomyocytes at day 21 for ELR and LOX. (n=2; 40x magnification; scale bar = 40 μ m)

4.2.4 Scanning electron microscopy

SEM images for each type of nanofiber scaffold are presented in **Figure 4.11**. Cardiomyocytes have anchored onto the PCL fibers in each scaffold. While cell body was not aligned with fiber structure within controls, collagen I and fibronectin-coated PCL cultures, cells seemed perfectly aligned along the longitudinal axis of the fibers within laminin and collagen IV-coated nanofibers. This might partially explain the significantly higher cells survival within these two scaffolds compared to the controls, collagen IV and fibronectin coated cases.

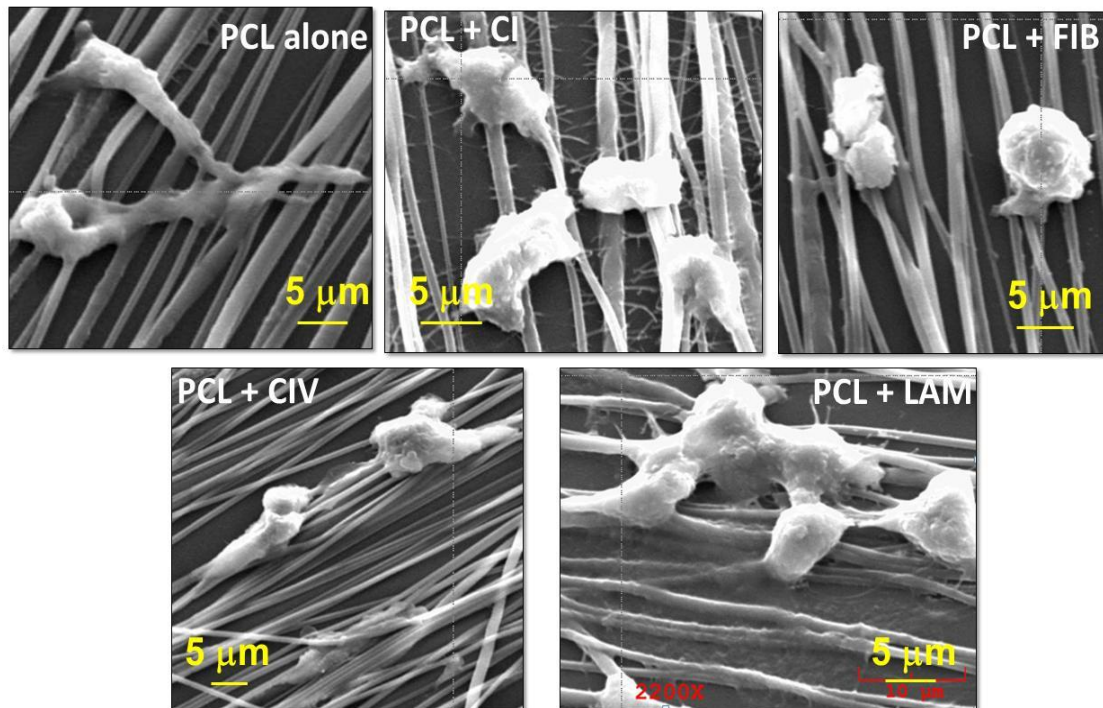


Figure 4.11 SEM images of rat cardiomyocytes cultured on PCL nanofiber scaffolds.

4.2.5 Beating cardiomyocytes

The rat cardiomyocytes expressed continuous contractile properties during the 21 day culture on the PCL nanofibrous scaffolds. The number of beating cells and their frequency was quantified and shown in **Figure 4.12**. The scaffold with uncoated PCL nanofibers exhibited the lowest percentage of beating myocytes with the lowest frequency. Furthermore, coating of these fibers allowed the cells to contract more and at a higher frequency. Although laminin coated PCL nanofiber scaffold provided the most suitable environment for cardiomyocytes to exhibit the highest number of beating cardiomyocytes, the contracting frequency was low. The highest beating frequencies were noted in cells cultured on collagen I and IV coated scaffolds. These contractile properties of cardiomyocytes could not be observed within hydrogels.

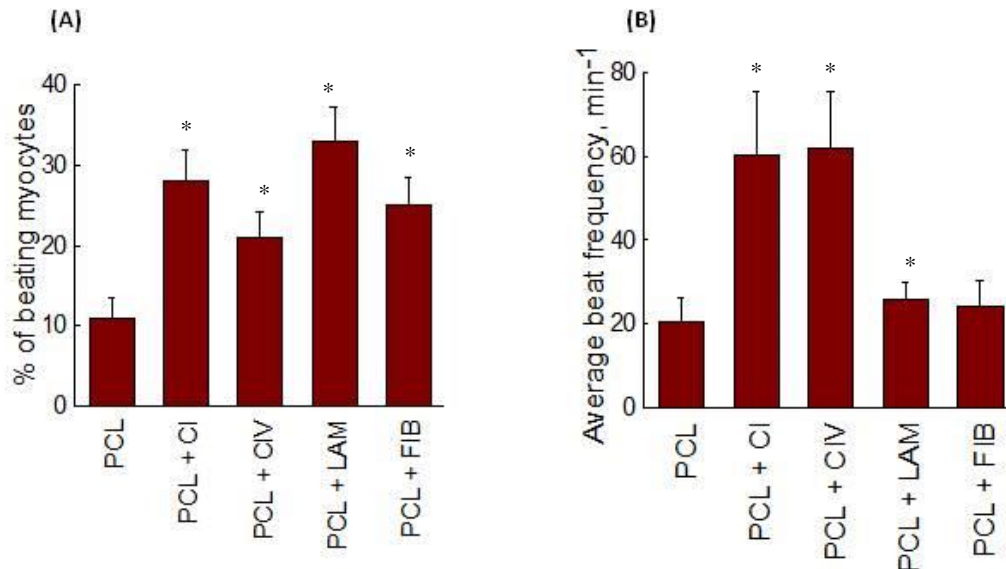


Figure 4.12 (A) Percentage of beating cardiomyocytes over the 21 day culture in five various scaffolds. (B) Average beating frequency of the cardiomyocytes during the 21 day culture.

CHAPTER V

CONCLUSIONS AND RECOMMENDATIONS

In this study, we developed and tested six types of 3D hydrogel scaffolds using the native proteins of ECM such as, collagen I, collagen IV, laminin and fibronectin. Additionally, we tested five different aligned PCL nanofibers scaffolds coated with the same proteins, including an uncoated PCL nanofiber plate as control. Although all these scaffolds have proved to be suitable for *in vitro* cardiomyocyte culture by providing cell attachment, survival, and cardiac phenotype expression, the amounts of ECM proteins synthesized by cardiomyocytes varied from scaffold to scaffold. The following are the conclusions from this study.

5.1 Conclusions

- ✧ Among all the hydrogels tested, collagen I at concentration of 2 mg/ml (CI-2) provided the highest cell survival rate and the lowest total protein content released in pooled media on a per cell basis.
- ✧ The increase of collagen concentration to 3 mg/ml resulted in a stiffer scaffold

decreasing cell survival. However collagen 3 mg/ml (CI-3) expressed the highest amount of sGAGs and elastin in both cell matrix and pooled media, as well as HA content in pooled media.

- ⤴ Opposite trends were noticed between elastin and LOX expression in pooled media. Given the fact that LOX cross-links tropoelastin monomers to form the elastin protein, the soluble tropoelastin collected in pooled media is found in higher content in cases where LOX expression is less and vice versa.
- ⤴ Overall, the highest total protein amount was synthesized by cardiomyocytes cultured in CI + CIV hydrogel. However, further studies at the genetic level are needed to understand how these hydrogels specifically upregulated synthesis and deposition of ECM proteins such as elastin, HA and sGAGs.
- ⤴ The collagen-I hydrogels (CI-1.2, CI-2 & CI-3) released low content of MMP-2 and TIMP-1, but drastically higher amounts of MMP-9. The addition of collagen-IV, or laminin, or fibronectin showed opposite trends by increasing MMP-2, TIMP-1 and reducing MMP-9.
- ⤴ Protein-coated PCL nanofibers provided better cell survival rate compared to uncoated PCL nanofibers, possibly due to lack of binding sites for cellular integrins to attach and home in.
- ⤴ While fibronectin-coated PCL nanofibers contributed to the highest total protein content in matrix as well as pooled media, collagen IV coating had the opposite effect. Interestingly, similar trends were noted in the amounts of protein deposited in matrix and released in pooled media, for all PCL nanofiber cases.
- ⤴ Cells cultured on laminin-coated PCL fibers expressed the largest content of

sGAGs and elastin whereas those cultured on collagen IV-coated fibers produced the highest amount of HA and LOX.

- ⤴ Hydrogels account for a much higher survival rate of cardiomyocytes compared to PCL nanofiber coated scaffolds. Among hydrogels, collagen 2 mg/ml is the most suitable scaffold for culturing cells (91% survival rate). In the cases of PCL nanofiber scaffolds, laminin-coating provided the best cell survival environment (42% survival rate).
- ⤴ In general, the total protein content quantified within PCL nanofiber scaffolds was significantly higher compared to that within hydrogels.
- ⤴ While sGAGs released in pooled media was significantly higher within hydrogels compared to that in PCL nanofiber coated scaffolds, nanofiber scaffolds facilitated higher fraction of sGAGs to be deposited as matrix. However, opposite trends was seen in HA synthesis.
- ⤴ Elastin synthesis was much higher in protein-coated PCL nanofibers compared to hydrogels.
- ⤴ TIMP-1 content in pooled media was the highest in fibronectin-coated PCL nanofibers, followed closely by laminin. The same outcome was noticed in hydrogels containing fibronectin or laminin (CI + FIB, CI + LAM).

5.2 Recommendations

The following are recommendations for future studies to further understand the effects of scaffolds on ECM protein production by cardiomyocytes and develop the most natural cardiac mimicking scaffold.

- ⤴ Semi-quantitative Western blot analysis to quantify elastin and LOX proteins within pooled media.
- ⤴ Enhance synchronized beating of cardiomyocytes within 3D scaffolds.
- ⤴ Develop an electrospinning setup to produce nanofibers blended with ECM proteins.
- ⤴ Quantify changes at the transcription-level (genetic level) for ECM protein synthesis and deposition within 3D scaffolds.

BIBLIOGRAPHY

1. Go AS, et al. Heart disease and stroke statistics--2013 update: A report from the American Heart Association. *Circulation*, 2013; 127: e6-245.
2. Bird SD, Doevendans PA, Van Rooijen MA, Brutel de la Riviere A, Hassink RJ, Passier R, & Mummery CL. The human adult cardiomyocyte phenotype. *Cardiovascular Research*, 2003;58(2): 423-434.
3. Kai D, Prabhakaran MP, Jin G, & Ramakrishna S. Guided orientation of cardiomyocytes on electrospun aligned nanofibers for cardiac tissue engineering. *Journal of Biomedical Materials Research Part B: Applied Biomaterials*, 2011; 98(2): 379-386.
4. Hosseinkhani H, Hosseinkhani M, Hattori S, Matsuoka R, & Kawaguchi N. Micro and nano-scale in vitro 3D culture system for cardiac stem cells. *Journal of Biomedical Materials Research Part A*, 2010; 94(1): 1-8.
5. Mitcheson JS, Hancox CJ, & Levi AJ. Cultured adult cardiac myocytes: Future applications, culture methods, morphological and electrophysiological properties. *Cardiovascular Research*, 1998; 39(2):280-300.
6. Zhang YZ, Venugopal J, Huang ZM, Lim CT, & Ramakrishna S. Characterization of the surface biocompatibility of the electrospun PCL-collagen nanofibers using fibroblasts. *Biomacromolecules*, 2005; 6: 2583-2589.
7. Shin M, Ishii O, Sueda T, & Vacanti JP. Contractile cardiac grafts using a novel nanofibrous mesh. *Biomaterials*, 2004; 25(17): 3717-3723.
8. Ho SY. Anatomy and myoarchitecture of the left ventricular wall in normal and in disease. *European Journal of Echocardiography*, 2008; 10(8): iii3-7.

9. Starling R, The Cleveland Clinic guide to heart failure. 2009.
10. Christman KL, & Lee RJ. Biomaterials for the treatment of myocardial infarction. *Journal of the American College of Cardiology*, 2006; 48(5): 907-913.
11. Jagtap P, & Szabo C. Poly (ADP-ribose) polymerase and the therapeutic effects of its inhibitors. *Nature Reviews. Drug Discovery*, 2005; 4: 421-440.
12. Swedberg K, et al. Guidelines for the diagnosis and treatment of chronic heart failure: executive summary—2005 update: The Task Force for the Diagnosis and Treatment of Chronic Heart Failure of the European Society of Cardiology. *European Heart Journal*, 2005; 26 (11): 1115-1140.
13. Schiele TM, Krotz F, & Klauss V. Vascular restenosis-striving for therapy. *Expert opinion on pharmacotherapy*, 2004; 5: 2221-2232.
14. Kelly ST, et al. Restraining infarct expansion preserves left ventricular geometry and function after acute anteroapical infarction. *Circulation*, 1999; 99: 135-142.
15. Borg TK, Rubin K, Lundgren E, Borg K, & Obrink B. Recognition of extracellular matrix components by neonatal and adult cardiac myocytes. *Developmental Biology*, 1984; 104: 86-96.
16. Lundgren E, Terracio L, Mardh S, & Borg TK. Extracellular matrix components influence the survival of adult cardiac myocytes in vitro. *Experimental Cell Research*, 1985; 158: 371-381.
17. Ruoslahti E. RGD and other recognition sequences for integrins. *Annual Review of Cell and Developmental Biology*, 1996; 12: 697-715.

18. Boateng SY, Lateef SS, Mosley W, Hartman TJ, Hanley L, & Russell B. RGD and YIGSR synthetic peptides facilitate cellular adhesion identical to that of laminin and fibronectin but alter the physiology of neonatal cardiac myocytes. *Am Journal of Physiology-Cell Physiology*, 2005; 288(1): C30-C38.
19. Prabhakaran MP, Venugopal J, Kai D, & Ramakrishna S. Biomimetic material strategies for cardiac tissue engineering. *Material Science and Engineering C*, 2011; 31: 503-513.
20. Kawaguchi N, Hatta K, & Nakanishi T. 3D-culture system for heart regeneration and cardiac medicine. *Biomed Research International* 2013; 1-6.
21. Evans HJ, Sweet JK, Price RL, Yost M, Goodwin RL. Novel 3D culture system for study of cardiac myocyte development. *American Journal of Physiology-Heart and Circulatory Physiology*, 2003; 285(2): H570-H578.
22. Zong X, Harold B, Chung C, Yin L, Fang D, Hsiao B, Chu B, & Entcheva E. Electrospun fine-textured scaffolds for heart tissue constructs. *Biomaterials*, 2005; 26(26): 5330-5338.
23. Sierra DH. Fibrin sealant adhesive systems: A review of their chemistry, material properties and clinical applications. *Journal of Biomaterials Applications*, 1993; 7:309-352.
24. Christman K, Fok HH, Sievers RE, Fang Q, & Lee RJ. Fibrin glue alone and skeletal myoblasts in a fibrin scaffold preserve cardiac function after myocardial infarction. *Tissue Engineering*, 2004; 10(3-4): 403–409.
25. Yu J, Gu Y, Du KT, Mihardja S, Sievers RE, & Lee RJ. The effect of injected RGD modified alginate on angiogenesis and left ventricular function in a

- chronic rat infarct model. *Biomaterial*, 2009; 30: 751-756.
26. Papavasiliou G, Sokic S, & Turturro M. Synthetic PEG hydrogels as extracellular matrix mimics for tissue engineering applications. *Biochemistry, Genetics and Molecular Biology*, 2012; chp 8.
 27. Dobner S, Bezuidenhout D, Govender P, Zilla P, & Davies N. A synthetic non-degradable polyethylene glycol hydrogel retards adverse post-infarct left ventricular remodeling. *Journal of Cardiac Failure*, 2009; 15(7): 629-636.
 28. Zimmermann WH, et al. Engineered heart tissue grafts improve systolic and diastolic function in infarcted rat hearts. *Nature Medicine*, 2006; 12 (4): 452–458.
 29. Miner EC, & Miller WL. A look between the cardiomyocytes: The extracellular matrix in heart failure. *Mayo Clinic Proceedings*, 2006; 81(1): 71-76.
 30. Pelouch V, Dixon IMC, Golfman L, Beamish RE, & Dhalla NS. Role of extracellular matrix proteins in heart function. *Molecular and Cellular Biochemistry*, 1994; 129: 101-129.
 31. Bashey RI, Martinez-Hernandez A, & Jimenez SA. Isolation, characterization, and localization of cardiac collagen type VI. Association with other extracellular matrix components. *Circulation Research*, 1992; 70: 1006-1017.
 32. Alberts B, et al. The extracellular matrix of animals. *Molecular Biology of the cell*, 2002.
 33. Weber KT, San Y, Tyagi SC, & Cleutjens JP. Collagen network of the

- myocardium: function, structural remodeling and regulatory mechanisms. *Journal of the American College of Cardiology*, 1994; 26(3): 279-292.
34. Bax N, Van Morion MH, Shah B, Goumans MJ, Bouten CV, Van der Schaft DW. Matrix production and remodeling capacity of cardiomyocyte progenitor cells during in vitro differentiation. *Journal of Molecular and Cellular Cardiology*, 2012; 53(4): 497-508.
 35. Sottile J, & Hocking DC. Fibronectin polymerization regulates the composition and stability of extracellular matrix fibrils and cell-matrix adhesions. *Molecular Biology of the Cell*, 2002. 13(10): 3546-59.
 36. Wagenseil JE, & Mechan RP. New insights into elastic fiber assembly. *Birth Defects Research Part C: Embryo Today*, 2007; 81(4): 229-240.
 37. Huynh MB, Morin C, Garpentier G, et al. Age-related changes in rat myocardium involve altered capacities of glycosaminoglycans to potentiate growth factor functions and heparan sulfate-altered sulfation. *Journal of Biological Chemistry*, 2012; 287(14): 11363-73.
 38. Wagenseil JE, & Mecham RP. Vascular extracellular matrix and arterial mechanics. *Physiological Reviews*, 2009; 89: 957-989.
 39. Fitzsimons CM, & Shanahan CM. Vascular extracellular matrix. *Pan Vascular Medicine: Integrated Clinical Management*, 1972; 217-226.
 40. Patel A, Fine B, Sandig M, & Mequanint K. Elastin biosynthesis: The missing link in tissue-engineered blood vessels. *Cardiovascular Research*, 2006; 71: 40-49.
 41. Ikonen L et al. Analysis of different natural and synthetic biomaterials to

support cardiomyocyte growth. *Journal of Clinical & Experimental Cardiology*, 2011; 1-7.

42. Pok S, Myers JD, Madihally SV, & Jacot JG. A multilayered scaffold of a chitosan and gelatin hydrogel supported by a PCL core for cardiac tissue engineering. *Acta Biomaterialia*, 2013; 9: 5630-5642.
43. Willitz RK, & Skornia SL. Effect of collagen gel stiffness on neurite extension. *Journal of Biomaterial Science: Polymer Edition*, 2004; 15(12): 1521-1531.